JCI The Journal of Clinical Investigation

Maternal diesel particle exposure promotes offspring asthma through NK cell-derived granzyme B

Qian Qian, Bidisha Paul Chowdhury, Zehua Sun, Jerica Lenberg, Rafeul Alam, Eric Vivier, Magdalena M. Gorska

J Clin Invest. 2020. https://doi.org/10.1172/JCI130324.

Research In-Press Preview **Immunology** **Pulmonology**

Graphical abstract

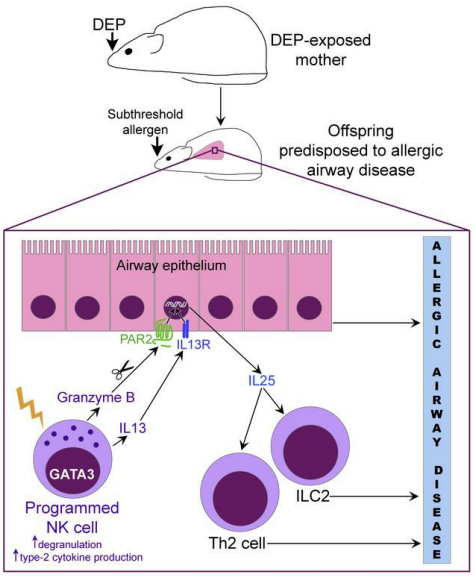

Maternal diesel particle exposure promotes offspring asthma through NK cell-derived granzyme B

Qian Qian[1], Bidisha Paul Chowdhury[1], Zehua Sun[1], Jerica Lenberg[1], Rafeul Alam[1, 2], Eric Vivier[3, 4, 5] and Magdalena M. Gorska[1, 2]

[1]Department of Medicine, Division of Allergy and Clinical Immunology, National Jewish Health, Denver, CO, 80206, USA

[2]Department of Medicine, Division of Allergy and Clinical Immunology, University of Colorado Anschutz Medical Campus, Aurora, CO, 80045, USA

[3]Innate Pharma Research Labs, Innate Pharma, Marseille, France

[4]Aix Marseille Univ, CNRS, INSERM, Centre d'Immunologie de Marseille-Luminy, Marseille, France

[5]Service d'Immunologie, Marseille Immunopole, Hôpital de la Timone, Assistance Publique des Hôpitaux de Marseille, France

Corresponding author: Magdalena M. Gorska, Department of Medicine, Division of Allergy and Clinical Immunology, National Jewish Health, 1400 Jackson St, Denver, CO, 80206, USA; Phone: 303.398.1656; Email: gorskam@njhealth.org

Conflict of interest: E.V. is a cofounder and employee of Innate Pharma. The other authors have declared that no conflict of interest exists.

Abstract

Mothers living near high-traffic roads before or during pregnancy have increased odds of having children with asthma. Mechanisms are unknown. Using a mouse model, here we showed that maternal exposure to diesel exhaust particles (DEP) predisposed offspring to allergic airway disease/AAD (murine counterpart of human asthma) through programming of their NK cells; predisposition to AAD did not develop in 'DEP' pups that lacked NK cells and was induced in normal pups receiving NK cells from wild type 'DEP' pups. "DEP' NK cells expressed GATA3 and co-secreted IL-13 and the 'killer' protease granzyme B in response to allergen challenge. Extracellular granzyme B did not kill but instead it stimulated protease-activated receptor 2 (PAR2) to cooperate with IL-13 in the induction of IL-25 in airway epithelial cells. Through loss-of-function and reconstitution experiments in pups, we showed that NK cells and granzyme B were required for IL-25 induction and activation of the type-2 immune response, and IL-25 mediated NK cell effects on type-2 response and AAD. Lastly, experiments using human cord blood and airway epithelial cells suggested that DEP might induce an identical pathway in humans. Collectively, we described an NK cell-dependent endotype of AAD that emerged in early life as a result of maternal exposure to DEP.

Introduction

A proportion of patients with asthma develop symptoms of their disease very early in life, sometimes in its first year (1). An early inception of a disease is usually linked to aberrant genes. However, genetics is unlikely to be the sole driver of asthma. Gene variants identified by GWAS studies are considered to account for only a small proportion of asthma prevalence (2). Studies on rare variants are predicted to offer only marginal improvement, leaving majority of asthma unexplained (2, 3). Therefore, it is now acknowledged that development of childhood asthma might be driven in substantial part by environmental exposures that children encounter either in utero or during their first years of life. Environmental impact on childhood asthma was underscored by seminal epidemiological studies that uncovered large differences in prevalence of childhood asthma between countries/regions with more vs. less Westernized lifestyles (4, 5). Building on this, other studies showed that childhood asthma positively correlated with exposure to urban air pollution and cigarette smoke and negatively, with exposure to the farming environment (6-9). Urban air pollution includes particulate matter (PM) generated by road traffic sources. The major constituents of traffic-related PM (up to 90%) are diesel exhaust particles (DEP) (6). There is considerable evidence that inhaled DEP directly harm children's lungs, activate their immune system, facilitate allergic sensitization and asthma inception (6, 8-10). More recent data, emerging from pregnancy cohort studies suggest that DEP may also act prenatally or even preconceptionally and have transgenerational effects (11, 12). The risk of childhood asthma increases if mothers live close to major roads and/or in areas with high levels of $PM_{2.5}$ ($PM \leq 2.5\mu m$) before and/or during pregnancy, or if DEP-linked biomarkers are found in the cord blood. This is an important problem; maternal exposures affect embryos and therefore may induce irreversible developmental damage and/or permanent long-lasting memory in offspring cells and tissues, potentially harming more than postnatal exposures. Prompted by human association studies, we used mouse models to show causative relationship between maternal exposure to DEP and offspring predisposition to allergic airway disease/AAD (murine counterpart of human asthma) (13, 14). Then, using these models, we began to study mechanisms. In this manuscript, we show that susceptibility to AAD in offspring of DEP-exposed mothers is due to emergence of a unique and unexpected pathway linking NK cells

and their protease granzyme B with activation of airway epithelial cells. The key outcome is IL-25 production by epithelial cells. NK cell-induced epithelial IL-25 activates pulmonary group-2 innate lymphoid cells (ILC2s) and Th2 cells, leading to AAD.

Results

Maternal exposure to DEP enhances the type-2 immune response in offspring

Using mouse models, we previously showed that maternal exposure to DEP either before or during pregnancy predisposed offspring to AAD (13, 14). For further studies, we chose the model with pre-pregnancy exposure. We favored it over its alternative with exposure during pregnancy because the former was more reflective of the human exposure that occurs randomly across the lifetime with no particular connection with pregnancy. In our chosen model, C57BL/6 female mice received six intranasal (i.n.) applications of DEP or PBS before pregnancy (see Supplemental Figure 1A for schematic illustration of the model). Two weeks after the final application, females were mated with unexposed males. Pups were sensitized to ovalbumin (OVA) to initiate the allergic response. Immunization included a single intraperitoneal (i.p.) injection of low dose OVA in alum on day 5 after birth. Separate sets of pups were injected with PBS. To elicit AAD, immunized pups were i.n. challenged with OVA on days 23, 24 and 25. Pups receiving PBS on day 5 were challenged with PBS. All pups were analyzed on day 28 after birth. The following groups of pups were studied: pups born to DEP mothers and exposed to PBS (DEP-PBS pups) or OVA (DEP-OVA pups) after birth, pups born to PBS mothers and exposed to PBS (PBS-PBS pups) or OVA (PBS-OVA pups) after birth. In PBS-OVA pups, AAD features (airway hyperresponsiveness (AHR) to methacholine, eosinophils in the bronchoalveolar lavage (BAL) fluid, peribronchial inflammation and goblet cell hyperplasia; ref. 13 and Figure 1A-C) were mild, reflecting immaturity of the neonatal immune system. Preconceptional DEP greatly exacerbated these features, leading to fully manifested AAD (ref. 13 and Figure 1A-C). To begin to address mechanisms of AAD intensification, we analyzed the type-2 immune response in the lung (Figure 1D-J). We found that among all studied groups of pups, DEP-OVA pups had the highest frequencies of IL-5^+ and IL-13^+ CD4 T cells in their lungs (Figure 1D, E) and the highest level of OVA-specific IgE in the serum (Figure 1F). DEP-OVA pups also had the highest frequencies of pulmonary IL25R^+ group 2 innate lymphoid cells/ILC2s ($CD45^+Lin^-CD127^+IL25R^+ST2^-$ cells and $CD45^+Lin^-CD127^+IL25R^+ST2^+$ cells ; Figure 1G, H), and the highest frequencies of pulmonary IL-5^+ and IL-13^+ ILC2s ($CD45^+Lin^-CD127^+$IL-5^+ cells and $CD45^+Lin^-CD127^+$IL-13^+ cells; Figure 1I, J). IL25R^+ ILC2s

and Th2 cells were also modestly increased in DEP-PBS pups (Figure 1E, H and J). IL25R-negative ILC2s ($CD45^+Lin^-CD127^+IL25R^-ST2^+$ cells) were not affected by maternal exposure to DEP (Figure 1G, H). Of note, our CD45/Lin/CD127/IL25R/ST2-based gating strategy accurately captured all ILC2s; $CD45^+Lin^-CD127^+IL25R^+ST2^-$ cells, $CD45^+Lin^-CD127^+IL25R^+ST2^+$ cells and $CD45^+Lin^-CD127^+IL25R^-ST2^+$ cells were also positive for other ILC2 markers such as GATA3, CD25 and ICOS, and $CD45^+Lin^-CD127^+IL25R^-ST2^-$ cells were negative or expressed very low levels of these markers (Supplemental Figure 1B).

Maternal signals prime offspring NK cells

ILC2s are not the only ILC subset in the lung. The most dominant subset, accounting for 10% pulmonary lymphocytes are NK cells. We asked whether the maternal influence extends to this ILC subset as well. DEP-OVA pups had more NK cells in the lung than PBS-OVA pups had (Figure 2A and Supplemental Figure 2A). Compared to pulmonary NK cells from PBS-PBS and PBS-OVA pups, pulmonary NK cells from DEP-PBS and DEP-OVA pups were more mature as illustrated by lower frequency of the $CD11b^-CD27^+$ subset and higher frequencies of $CD11b^+CD27^-$ (Figure 2B, C and Supplemental Figure 2A), $CD11b^+CD27^-KLRG1^+$ and $CD11b^+CD27^-KLRG1^+Ly6C^+$ (Figure 2D and Supplemental Figure 2A) subsets. Downregulation of CD27 and induction of CD11b, KLRG1 and Ly6C are indicative of terminal maturation, development of NK cell memory, and predictive of enhanced effector functions (15, 16). Indeed, pulmonary NK cells from pups of DEP exposed mothers showed increased degranulation, denoting increased secretion of granule proteins including granzymes (DEP-OVA pups, Figure 2E), and enhanced capacity to produce IL-5 and IL-13 (DEP-PBS and DEP-OVA pups, Figure 2F). This was intriguing because NK cells are not generally thought to secrete type-2 cytokines; instead they are the major sources of type-1 cytokines such as IFNγ. Particularly interesting was production of IL-5 and IL-13 by DEP-PBS NK cells. The result suggested that DEP-linked signals have capacity to induce type-2 differentiation program in NK cells. In support of this hypothesis, DEP-PBS NK cells showed increased expression of the transcriptional master-regulator of the type-2 polarization program, GATA3 (Figure 2G). Collectively, our data indicated that maternal exposure to DEP imprinted a pro-allergic maturation program in offspring NK cells.

NK cells drive the type-2 immune response and allergic airway disease

We were intrigued by NK cell activation in our model, because NK cells are not traditionally believed to participate in asthma/AAD. We decided to investigate this further. To study importance of NK cells in type-2 response and AAD, we took three approaches. In the first approach, we used the $Ncr1^{iCre}R26^{DTA}$ model of NK cell deficiency (17). The $Ncr1^{iCre}$ knock-in allele has the *YFP-IRES-Cre* cassette inserted into the 3' untranslated region of the *Ncr1* gene (encoding the NKp46 protein), enabling coordinated transcription of *Cre* and endogenous *Ncr1*. *Ncr1* is one of the most specific genes of the NK cell lineage (17, 18). In our model, 91.36±1.42% of lung NKp46$^+$ cells expressed NK1.1 and lacked CD3 fitting into the traditional definition of NK cells (Supplemental Figure 2B). Thus, our results confirmed previous reports on the high degree of co-expression between NKp46 and other markers of NK cells, supporting the choice of $Ncr1^{iCre}$-based strategy for deletion of NK cells. The other element of the NK cell deletion strategy is the $R26^{DTA}$ allele. This allele has the diphtheria toxin A (*DTA*) gene and the upstream loxP-flanked STOP codon inserted into the ubiquitously-expressed *ROSA26* locus. STOP codon prevents *DTA* transcription. A cross of $Ncr1^{iCre}$ to $R26^{DTA}$ mice enables excision of STOP by Cre and transcription of *DTA* in NKp46$^+$ cells. As a result, NKp46$^+$ cells are killed leaving other cells intact. In our experiment, DEP-exposed $Ncr1^{iCre/+}$ mothers were mated with unexposed $R26^{DTA/DTA}$ fathers to generate NK cell-deficient $Ncr1^{iCre/+}R26^{DTA/+}$ and NK cell-sufficient $R26^{DTA/+}$ littermates. All pups were immunized and challenged with OVA. $Ncr1^{iCre/+}R26^{DTA/+}$ pups lacked NK cells but had normal frequencies of NKT cells and conventional CD3$^+$NK1.1$^-$ T cells (Supplemental Figure 2C, D). NK cell deficiency led to marked reduction in pulmonary IL-5 and IL-13 (Figure 3A, B), IL25R$^+$ and type-2 cytokine$^+$ ILC2s (Figure 3E, F), IL-5$^+$ and IL-13$^+$ CD4 T cells (Figure 3C), OVA-specific IgE in the serum (Figure 3D) and all features of AAD, including airway hyperresponsiveness (AHR) to methacholine (Figure 3G, Supplemental Figure 2E), eosinophils (Figure 3I, Supplemental Figure 2F), peribronchial inflammation (Figure 3H) and goblet cell hyperplasia (Figure 3J).

In addition to being expressed by NK cells, NKp46 is also detected on few rare lymphocyte subsets such as ILC1s, NKp46$^+$ ILC3s and a minute fraction of NKT cells. Consistent with this, $Ncr1^{iCre/+}R26^{DTA/+}$ mice lack ILC1s and NKp46$^+$ ILC3s (19). To assure that the observed effects of NKp46$^+$ cells on AAD represented effects

of conventional NK cells and not the effects of NKp46$^+$ ILC1/ILC3/NKT cells, we performed two experiments. Conventional NK cells can be distinguished from ILC1/ILC3s and NKT cells by expression of CD127 and CD3 by ILC1/ILC3s and NKT cells, respectively. Building on this, to exclude roles of NKp46$^+$ ILCs and NKT cells, we reconstituted *Ncr1*$^{iCre/+}$*R26*$^{DTA/+}$ pups with CD127$^-$ NK cells (see Supplemental Figure 3B for diagram of the experimental strategy). To purify CD127$^-$ NK cells, we used the negative selection-based Miltenyi NK Cell Isolation Kit that included anti-CD3, and was additionally supplemented by us with anti-CD127. The purified cell population was devoid of NKT cells (NK1.1$^+$CD3$^+$), ILC1s (CD45$^+$Lin$^-$CD127$^+$Eomes$^-$T-bet$^+$NKp46$^+$), NKp46$^+$ and NKp46$^-$ ILC3s (CD45$^+$Lin$^-$CD127$^+$ RORγt$^+$NKp46$^+$ and CD45$^+$Lin$^-$CD127$^+$ RORγt$^+$NKp46$^-$) and ILC2s (CD45$^+$Lin$^-$CD127$^+$NKp46$^-$GATA3$^+$) (Supplemental Figure 3A). Transfer of CD127$^-$ NK cells from NK cell-sufficient DEP-OVA pups into NK cell-deficient *Ncr1*$^{iCre/+}$*R26*$^{DTA/+}$ DEP-OVA pups led to complete reconstitution of IL25R$^+$ ILC2s (Figure 3K) and features of AAD (Figure 3L-N), supporting our conclusions on dependence of these traits on conventional NK cells and underscoring lack of meaningful involvement of NKp46$^+$ ILC1/ILC3s and NKT cells.

Lastly, we used the anti-asialo-GM1 antiserum to deplete NK cells (diagram of the experimental strategy in Supplemental Figure 3C). Anti-asialo-GM1 does not delete ILC1/ILC3s and NKT cells (ref: 20, 21; Supplemental Figure 3D). Pups of DEP-exposed mothers were injected with the anti-asialo-GM1 antiserum one day before immunization, one day before challenge and on the last day of challenge. Anti-asialo-GM1 reduced all features of AAD (Figure 3O-Q).

The type-2 immune response and allergic airway disease are dependent on IL-25

We previously showed that airway inflammation and AAD in our model were dependent on IL-1β and its downstream target IL-17A that mediated airway hyperresponsiveness (13). IL-1β is a recognized enhancer of the type-2 immune response, activating both ILC2s and Th2 cells. We thus wondered whether IL-1β and NK cells are linked. *Ncr1*$^{iCre/+}$*R26*$^{DTA/+}$ and *R26*$^{DTA/+}$ DEP-OVA littermates did not differ in regard to levels of mRNA for IL-1β and IL-17A, indicating that NK cells did not control these cytokines (Supplemental Figure

4A). We also tested whether the opposite is true i.e. whether IL-1β regulated NK cells. To this end, DEP-OVA pups were injected with a neutralizing anti-IL-1β antibody (or control IgG) on postnatal day 5 (one day before immunization) and then on postnatal day 22 (one day before the first challenge with OVA; diagram of experimental strategy in Supplemental Figure 4B). Although this treatment depleted IL-1β (Supplemental Figure 4C) and prevented development of AAD in our previous study (13), it had no effect on NK cell maturation (Supplemental Figure 4D, E), degranulation (Supplemental Figure 4F) and type-2 cytokine production (Supplemental Figure 4G). Taken together, our data indicated that IL-1β and NK cells are not linked and therefore they regulate type-2 inflammation and AAD through independent routes.

Having established that NK cells were unlikely to activate ILC2s and Th2 cells through IL-1β (Supplemental Figure 4A), we shifted our focus to more traditional regulators of these cells i.e. epithelial cytokines IL-25, IL-33 and TSLP. At 72 hours after challenge with OVA, DEP-OVA pups over-expressed and over-secreted IL-25 (Figure 4A, B) and expressed and secreted normal levels of IL-33 and TSLP (Figure 4A, B) in their lungs. We reasoned that IL-25 induction could explain expansion of IL-25R$^+$ ILC2s. To examine importance of IL-25 in IL25R$^+$ ILC2 activation, other features of the type-2 immune response and AAD, DEP-OVA pups were injected with an IL-25-depleting antibody one day before immunization, and then one day before the first challenge with OVA (see Supplemental Figure 4B for diagram of the experimental strategy). The anti-IL-25 antibody reduced pulmonary IL25R$^+$ ILC2s (Figure 4C), OVA-specific IgE in the serum (Figure 4D) and features of AAD (Figure 4E-H, Supplemental Figure 4H, I) to levels comparable to those in PBS-OVA pups. Of note, IL-25 depletion had no effect on IL-1β and IL-17A (Supplemental Figure 4J). In conclusion, IL-25 was an important driver of DEP-programmed, allergen-elicited type-2 inflammation and AAD.

Normal levels of IL-33 and TSLP mRNAs and proteins were somewhat surprising, given importance of these cytokines for lung inflammation in other models of allergic airway disease. To obtain definitive answers on contributions of IL-33 and TSLP to AAD in our model, we individually depleted these cytokines in DEP-OVA pups using specific antibodies (diagram of experimental strategy in Supplemental Figure 4B). Separate groups of pups received control IgGs. Injections of anti-IL-33 and anti-TSLP antibodies led to substantial reductions of

targeted cytokines (Figure 4I, M) but had no effect on AAD (Figure 4J-L and 4N-P), indicating that IL-33 and TSLP were redundant in our model. These results were consistent with lack of DEP effects on IL-25R^{-}ST2^{+} ILC2s (Figure 1H).

NK cells are upstream of IL-25

We asked whether IL-25 and NK cells are linked. To study the effect of NK cells on IL-25, we used NK cell deficient pups. NK cell deficiency led to marked reduction of pulmonary IL-25 mRNA and protein (Figure 5A-C). The loss of IL-25 was most evident in airway epithelial cells (Figure 5C). These cells were the principal sources of IL-25 in control pups. NK cell deficiency did not affect IL-33 and TSLP, suggesting relative selectivity of NK cells for IL-25 (Figure 5A, B).

We then wanted to determine whether or not IL-25 induction was the key mechanism responsible for induction of the type-2 immune response and AAD by NK cells. To test this, *Ncr1*$^{iCre/+}$*R26*$^{DTA/+}$ pups of DEP-exposed mothers were administered with recombinant IL-25 during the immunization phase (on postnatal days 5 and 6), and then during the challenge phase (on postnatal days 23, 24 and 25) (diagram of the experimental strategy in Supplemental Figure 5). IL-25 reconstitution led to restoration of pulmonary IL25R^{+} ILC2s (Figure 5D) and AAD (Figure 5E-G), indicating that IL-25 induction was critical for NK cell regulation of these traits. Therefore, NK cells promoted the type-2 response and AAD via IL-25.

NK cells serve as carriers of susceptibility to allergic airway disease

To test whether NK cells are carriers of AAD predisposition in our model, we transferred CD127^{-} NK cells from wild type pups of DEP and PBS exposed mothers (referred to as DEP NK cells and PBS NK cells, respectively) into normal (no DEP) age-matched recipients (diagram of the experimental strategy in Supplemental Figure 6, see protocol #1). The third group of recipients was injected with PBS without cells. All recipients were born to unexposed mothers and had the *Ncr1*$^{iCre/+}$*R26*$^{DTA/+}$ (NK cell-null) genotype. Intratracheal (i.t.) transfer took place at three weeks of age, after neonatal (postnatal day 5) immunization of recipients. Donors were not immunized. Following NK cell transfer/PBS injection, recipients were challenged

with OVA. PBS-injected recipients had low level of IL-25 in the BAL fluid (Figure 6A), low numbers of $IL25R^+$ ILC2s (Figure 6B) and minimal AAD (Figure 6C, D), reflecting immaturity of the immune system at the time of immunization. Transfer of PBS NK cells did not have any effects on these traits. In contrast, transfer of DEP NK cells led to increased production of IL-25, expansion of $IL25R^+$ ILC2s and exacerbation of AAD. Thus, DEP NK cells were programmed to promote the type-2 immune response and AAD. This program made them sufficient to transmit AAD susceptibility to normal recipients. We then asked whether the DEP-linked program persisted in the NK cell lineage beyond the early postnatal life, into the adulthood. To address this, we used adult (6-week old) offspring of DEP-exposed and PBS-exposed mothers as NK cell donors (Supplemental Figure 6, protocol #2). The overall experimental design was same as that used for 3-week old donors - NK cells (or PBS) were i.t. transferred into immunized aged-matched (6-week old) NK cell-deficient recipients. Immunization (a single i.p. dose of OVA in alum) took place seventeen days prior to NK cell/PBS injection. One day following NK cell /PBS injection, recipients underwent their first challenge with OVA. Compared to recipients of PBS NK cells and recipients of PBS, recipients of DEP NK cells had increased IL-25 in the BAL fluid (Figure 6E), increased numbers of pulmonary $IL25R^+$ ILC2s (Figure 6F) and showed exacerbation of AAD (Figure 6G, H). The result highlighted persistence of NK cell programming into the adulthood. In addition, the result indicated that after achieving maturity and transitioning into adulthood, the lung remained amenable to signals emitted by DEP NK cells, continuing to respond by mounting type-2 inflammation and AAD.

NK cell dominance is unique to maternal DEP-programmed allergic airway disease

We then explored whether or not NK cell participation was a general feature of AAD. To this end, we performed two experiments. In the first experiment, we used normal (no maternal DEP) adult mice and the conventional OVA-based model of AAD (diagram of the experimental strategy in Supplemental Figure 7). Experimental mice were adult offspring of unexposed $Ncr1^{iCre/+}$ mothers and $R26^{DTA/DTA}$ fathers. In this model, $Ncr1^{iCre/+}R26^{DTA/+}$ and $R26^{DTA/+}$ adult littermates had similar numbers of lung ILC2s (Figure 7A) and same magnitude of AAD (Figure 7B-E). Our results agreed with the recently published study that also used

Ncr1^{iCre}*R26*^{DTA} mice to show lack of any meaningful involvement of NK cells in adult OVA- and HDM-based models of AAD (22). Taken together, NK cells are redundant for allergen-driven DEP-free AAD in adult mice. We then examined NK cell engagement in an early-life model of allergen-driven AAD. We address this by subjecting *Ncr1*$^{iCre/+}$ mothers and their *Ncr1*$^{iCre/+}$*R26*$^{DTA/+}$ and *R26*$^{DTA/+}$ neonates to our PBS-OVA exposure scheme (Supplemental Figure 1A). As discussed earlier, in PBS-OVA pups, due to immaturity of their immune system, immune responses are of low magnitude; nevertheless, these pups develop low-grade airway eosinophilia and AHR that clearly differentiate them from PBS-PBS pups (13). As was the case with the adult model, numbers of ILC2s (Figure 7F) and eosinophils (Figure 7H), AHR (Figure 7G) and other AAD features (Figure 7I, J) in PBS-OVA *Ncr1*$^{iCre/+}$*R26*$^{DTA/+}$ pups were same as these in PBS-OVA *R26*$^{DTA/+}$ pups. By comparing results of this experiment with data in Figure 3G-J, we also noted that AAD features in NK cell-sufficient/deficient PBS-OVA pups were approximately of the same level as AAD features in NK cell-deficient DEP-OVA pups. Altogether, our results indicated that NK cell engagement in AAD was not merely a consequence of allergen exposure or young age of pups, but a consequence of maternal exposure to DEP.

The NK cell granule protease granzyme B induces IL-25 in airway epithelial cells

IL-13 is a recognized inducer of epithelial IL-25 (23), providing one potential link between NK cells and IL-25. However, IL-13 can be produced by other cells, suggesting that requirement for NK cells in AAD is imposed by another mediator(s) that is more specific to NK cells. In search of these mediators, we analyzed previously-published NK cell transcriptome data (15, 18, 24), selected mRNAs with links to airway epithelial cells, the lung, asthma, or type-2 immunity and measured them in lungs of DEP-OVA *Ncr1*$^{iCre/+}$*R26*$^{DTA/+}$ and *R26*$^{DTA/+}$ littermate pups (Figure 8A). None of these mRNAs was affected by NK deficiency, suggesting greater importance of other cellular sources. In contrast, NK cell-related mediators of cytotoxicity i.e. the proteases granzyme A, granzyme B and cathepsin W were markedly reduced. A large reduction of granzymes indicated that NK cells were their primary source. Indeed, NK cells accounted for 88.28±0.99% of granzyme B^{+} cells in lungs of DEP-OVA pups (Figure 8B). This was consistent with previous reports comparing granzyme levels in NK cells vs. CD8 T cells. NK cells have much higher expression of granzymes at baseline as part of their

persistently ‘alert’ state (18). CD8 T cells require stimulation to induce granzymes. This stimulation was perhaps insufficient in our model.

We tested whether granzymes and cathepsin W could directly stimulate airway epithelial cells to produce IL-25. To this end, we incubated C57BL/6 mouse primary airway epithelial cells (for purity, see Supplemental Figure 8A) with or without recombinant mouse granzyme A, granzyme B or cathepsin W ± IL-13, or with an extract of an allergen Alternaria alternata (positive control) (Figure 8C, D). The Alternaria extract is a well-established activator of airway epithelial cells, inducing release of several pro-inflammatory mediators, including IL-25. Granzyme B induced IL-25 (Figure 8C, D). Furthermore, granzyme B potentiated the effect of IL-13 on IL-25, highlighting cooperation between these two NK cell-expressed epithelial activators. Experiments using small molecule inhibitors indicated that granzyme B-mediated IL-25 induction was dependent on the protease-activated receptor 2 (PAR2), emphasizing importance of granzyme B proteolytic activity (Figure 8E). The inhibitor experiment also pointed to substrate selectivity of the granzyme B protease, action of which was not dependent on another member of the PAR family - PAR1. Granzyme A and cathepsin W did not have any effects on IL-25. This was consistent with previous reports showing that granzyme A, granzyme B and cathepsin W differ in their substrate specificities (25). None of the proteases affected IL-33 and TSLP. In control experiments, we determined that all proteases were enzymatically active (Supplemental Figure 8B), indicating that inability of granzyme A and cathepsin W to induce IL-25 was not due to absence of their proteolytic activity. We also determined that none of the proteases induced cell death (Figure 8F), excluding a possibility of death-related release of IL-25. Lack of cell death was consistent with an established paradigm on requirement of perforin and intracellular delivery for granzyme-mediated cell death (death-related substrates of granzymes (caspases) are intracellular) (26). Our culture system did not include perforin. Altogether, we identified granzyme B as an inducer of IL-25 in airway epithelial cells. Granzyme B showed relative selectivity towards IL-25, as IL-33 and TSLP were not affected by its action. Our data confirmed previous observations on differences in regulation of these cytokines (27-32). To exemplify this, IL-33 is constitutively expressed at a high level by various epithelial cells from multiple organs, endothelial cells of high endothelial venules (HEV) and fibroblastic reticular cells (FRC) of lymph nodes and spleen (27). Within pulmonary epithelium, IL-33 is

primarily expressed by human basal cells and mouse alveolar type-2 cells. Constitutive expression of IL-25 is limited to tuft cells, a rare epithelial subset that is seen in the gut, upper airways and trachea but not in the distal airways and the lung (28-30); other cells, including bronchial epithelial cells require environmental stimulation to produce IL-25. The dominant mechanism by which IL-33 is released from cells is necrosis. Only few stimuli are known to liberate IL-33 from living cells and these include the Alternaria extract (working via coordinated activation of multiple receptors and pathways), ATP and mechanical stress (31, 32). In contrast, IL-25 secretion can be elicited by less complex stimuli such as cytokines (ref: 23 and Figure 8D).

NK cells promote IL-25 production through direct effects on the airway epithelium

Our experiments indicated that at least two NK cell mediators (the granule protease granzyme B and IL-13) had the capacity to directly act on the airway epithelium and induce IL-25. We thus wondered whether induction of IL-25 by NK cells occurred through their direct effects on epithelial cells. To answer this question, we set up an in vitro co-culture system using normal C57BL/6 airway epithelial cells (as in Figure 8C-F) and NK cells that were isolated from spleens of DEP-OVA pups. DEP-OVA NK cells induced the IL-25 protein in epithelial cells (Figure 8G).

Granzyme B is required for development of allergic airway disease in predisposed pups

We next asked whether granzyme B was important for development of AAD in our model. To this end, we performed two experiments. In the first experiment, we studied the role of systemic granzyme B. DEP-exposed females heterozygous for knockout mutation in the granzyme B gene (*Gzmb*$^{-/+}$) were mated with unexposed *Gzmb*$^{-/+}$ males to produce *Gzmb*$^{-/-}$ and *Gzmb*$^{+/+}$ littermate pups. Pups were immunized and challenged with OVA, per our regular protocol. Compared to *Gzmb*$^{+/+}$ pups, *Gzmb*$^{-/-}$ pups had less IL-25 and IL25R^{+} ILC2s in their lungs (Figure 9A, B) and reduced AAD (Figure 9C-F). In the second experiment, we explored the role of NK cell-expressed granzyme B (diagram of the experimental strategy in Supplemental Figure 9). This was accomplished through transfer of *Gzmb*$^{-/-}$ and control *Gzmb*$^{+/+}$ CD127^{-} NK cells into NK cell-deficient recipients. Donor *Gzmb*$^{-/-}$ and *Gzmb*$^{+/+}$ pups were littermates born to *Gzmb*$^{-/+}$ parents. Recipient pups came from

the cross of *Ncr1*$^{iCre/+}$ mothers and *R26*$^{DTA/DTA}$ fathers. Both sets of mothers (generating either donors or recipients) received DEP. Prospective donor and recipient pups were immunized with OVA in alum on postnatal day 5. NK cell transfer (i.t. route) took place on postnatal day 22. After transfer, recipients were challenged with OVA. Compared to recipients of *Gzmb*$^{+/+}$ NK cells, recipients of *Gzmb*$^{-/-}$ NK cells had less IL-25 and IL25R^{+} ILC2s (Figure 9G, H) and decreased AAD (Figure 9I-L). In conclusion, NK cell-expressed granzyme B was required for elicitation of AAD in predisposed pups. Absence of granzyme B specifically in NK cells yielded similar effects on AAD as the absence of systemic granzyme B. This was consistent with NK cells being the dominant source of this protease in our model (Figure 8B).

Granzyme B is required for the direct effect of NK cells on epithelial cells

We next asked whether granzyme B mediated the direct effect of NK cells on airway epithelial cells. To address this, we again employed our NK-epithelial co-culture system but this time used *Gzmb*$^{-/-}$ and *Gzmb*$^{+/+}$ NK cells. NK cells were isolated from spleens of DEP-OVA *Gzmb*$^{-/-}$ and *Gzmb*$^{+/+}$ littermates. Compared to *Gzmb*$^{+/+}$ NK cells, *Gzmb*$^{-/-}$ NK cells had reduced capacity to induce IL-25 (Figure 9M) in airway epithelial cells, highlighting importance of the protease in mediating direct effects of NK cells.

DEP-programmed NK cells drive the type-2 immune response and AAD to the clinically-relevant house dust mite allergen

In our final experiments we tested whether the NK cell-dependent pathway was operational and important in the human-relevant context. To address this, we used a clinically-relevant allergen to elicit AAD in mice and employed human cell culture systems. In the first experiment we examined whether offspring responses to human allergen were impacted by maternal exposure to DEP. To this end, pups of DEP-exposed or PBS-exposed mothers were sensitized with an intranasal application of the house dust mite extract (HDM) on postnatal days 5 and 6 followed by three intranasal challenges with HDM on days 23, 24 and 25 and analysis on day 28 (diagram of experimental strategy in Supplemental Figure 10). PBS-HDM pups displayed weak type-2 immune response (Figure 10B-E) and low-level AAD (Figure 10F-H), as expected from normal unprimed (no

maternal exposure) neonates. The type-2 immune response and AAD were considerably enhanced in DEP-HDM pups (Figure 10B-H). This was linked to increased expression of type-2 cytokines by pulmonary NK cells (Figure 10A). Therefore, maternal exposure to DEP facilitated allergic response to HDM in offspring. In the second experiment, we asked whether HDM-elicited AAD was dependent on NK cells. Compared to $R26^{DTA/+}$ pups of DEP-exposed mothers, their NK cell deficient $Ncr1^{iCre/+}R26^{DTA/+}$ littermates had reduced type-2 immune response (Figure 10I-L) and AAD (Figure 10M-O), indicating that DEP-programmed NK cells are critical drivers of AAD in the HDM context.

DEP promote degranulation and type-2 cytokine production by human cord blood NK cells

In the third experiment, we asked whether DEP could regulate functions of human early-life NK cells. To test this, we measured NK cell activation in DEP-stimulated cultures of human cord blood mononuclear cells (CBMCs). Control cultures were stimulated with HDM or treated with a vehicle (PBS). DEP promoted NK cell degranulation (i.e. secretion of granzyme B; Figure 11A, B, E), and NK cell production of type-2 cytokines IL-4 and IL-5 (Figure 11C, D, F, G). IL-13 was undetectable in this system (Figure 11D). DEP had no effect on NK cell production of IFNγ (Figure 11H). HDM did not influence any of the NK cell activation parameters (Figure 11A-H). These results suggested that DEP endowed human early-life NK cells with the capacity to stimulate airway epithelial cells (via granule-derived granzyme B and IL-4 that shares its epithelial receptor with IL-13) and other cells involved in the type-2 response such as CD4 T cells, ILC2s, B cells and eosinophils (via IL-4 and IL-5). HDM did not have these effects on NK cells, which was consistent with our mouse data (Figure 7) showing that NK cells did not participate in AAD elicited by an allergen alone i.e. in the absence of DEP.

Human granzyme B stimulates human airway epithelial cells to produce IL-25

In the final experiment, we examined effects of human recombinant granzyme B on human primary airway epithelial cells in the in vitro culture model. Human granzyme B induced transcription of the *IL25* gene (Figure 11I). The granzyme B effect on *IL25* was enhanced by the IL4Rα/IL13Rα1 ligand - IL-13. Granzyme B had no

effect on *IL33*. Collectively, these results reflected our data obtained using the mouse epithelial culture system (Figure 8C, D).

Discussion

Asthma is a heterogeneous disease that encompasses multiple endotypes (distinct mechanistic variants). Emergence of a particular endotype is dictated by several factors, including genotype, gender, environmental exposures and age/developmental period when these exposures occur. Using a mouse model, we described an NK cell-dependent endotype of allergic airway disease (AAD, murine counterpart of human asthma) that arose in early life as a result of maternal exposure to DEP. We then showed that NK cells induced AAD via activation of airway epithelial cells. NK cell-derived granzyme B directly stimulated the epithelium to produce IL-25. Granzyme B-mediated induction of IL-25 was enhanced by IL-13 that is co-secreted by NK cells. NK cell-induced epithelial IL-25 activated ILC2s and Th2 cells, leading to eosinophilic inflammation of airways and AAD. Lastly, experiments using human cord blood and human airway epithelial cells suggested that DEP might induce an identical pathway in humans.

In fact, there is some evidence in prior literature that the NK cell-linked, early-onset endotype of asthma does indeed exist in humans. One recent study showed that inner-city children who developed allergic asthma by age 7 were distinguished from children who did not develop asthma by higher levels of NK cell-related transcripts in PBMCs at age 2, i.e. in a period prior to asthma manifestation (33). The list of the most significantly upregulated genes included granzyme B. Since inner-city children are exposed to high levels of air pollution, including DEP, this study gave a hint on a potential link between DEP and NK cells in humans. Air pollution-triggered activation of NK cells may persist beyond early childhood, as indicated by another study that detected increased levels of NK cell-related transcripts (including transcript for granzyme B) in PBMCs of inner-city asthmatics at age 8-11 (34).

Previous reports also support connection between early-life asthma and IL-25. Rhinovirus (RV) infection is an important trigger of asthma in young children. RV promotes asthma partly via activation of the airway epithelium. A recent study showed that induction of epithelial IL-25 by RV was age-dependent occurring only

in neonates but not in adult mice (35). RV-triggered IL-25 drove neonatal AAD. Given our results and the established paradigm placing NK cells as key responders to viruses, we speculate that IL-25 induction in RV-infected neonates is driven by NK cells. Therefore, RV-induced neonatal asthma may be another asthma endotype that depends on NK cells.

In addition to predicting another endotype of asthma, our study has a potential to pave the way for development of diagnostic tests for early detection of asthma predisposition. We postulate that these tests should measure type-2 cytokine^{+} NK cells, granzyme B and IL-25. Currently, cord blood IgE is the only biomarker with a potential to predict future allergic disease (36). However, IgE may not capture an innate component of asthma predisposition e.g. priming of ILC2s. NK cells act upstream of both innate (ILC2s) and adaptive (Th2s/IgE) arms of the type-2 immune response. We thus propose that measurements of NK cell-linked biomarkers could complement IgE tests, being particularly useful in cases when IgE is negative. NK cell biomarkers are also potentially more sensitive in detecting early changes than ILC2 markers. It is because NK cells act upstream of ILC2s. Lastly, because ILC2 counts are extremely low in the blood, measurements of NK cell-linked markers are significantly more practical.

Our study has implications for understanding basic mechanisms of the immune response. NK cells are traditionally viewed as cytotoxic cells that kill dangerous "non-self" targets such as virally-infected and transformed cells. More recent data indicate that NK cells can affect normal cells, including cells of the immune system. By secreting IFNγ and TNFα, NK cells contribute to activation of dendritic cells, macrophages and T cells, and induction of the type-1 immune response (37). NK cells also take part in resolution of the type-1 response through killing of participating immune cells (37). Much less is known about NK cell effects on the type-2 response. There are reports on type-2 cytokine-producing NK cells in human asthma (38) but significance of this for asthma has never been addressed. NK cells can kill eosinophils in vitro, suggesting that in some circumstances, NK cells may participate in resolution of allergic inflammation (39). Here we show that

in the context of maternal DEP, NK cells become key drivers of the type-2 immune response, allergic inflammation and AAD.

Granzyme B is best known for its capacity to kill target cells. This occurs after its intracellular delivery via cleavage and activation of pro-apoptotic caspases (25, 26). More recent reports indicate that granzyme B may also have non-cytotoxic functions. Granzyme B cleaves extracellular matrix proteins and thereby facilitates chemokine-induced movement of cytotoxic lymphocytes through basement membranes (40). Furthermore, granzyme B amplifies LPS-induced TNFα release from human monocytes in vitro (41). Lastly, granzyme B cleaves IL-1α, enhancing its biological activity (42). It remains to be established whether granzyme B-mediated TNFα release and IL-1α cleavage occur in vivo, and whether these processes are important for inflammation and development of diseases. There are no reports that define specific functions of granzyme B in type-2 inflammation. Our manuscript is an opening act in pursuit of this question. Intriguingly, granzyme B-triggered mechanism that we uncovered resembles some of the mechanisms that are elicited by allergens. House dust mite and pro-allergic fungi (Alternaria and Aspergillus) contain proteases and induce asthma partly via PAR2-mediated activation of the airway epithelium (43).

The lung has the highest frequency of NK cells (≈10% of lymphocytes) among all non-lymphoid and lymphoid organs (44), suggesting that NK cells play special roles in the lung. NK cells defend against respiratory infections and destroy cigarette smoke-damaged epithelial cells in chronic obstructive pulmonary disease (COPD) (45, 46). Whether NK cells have other functions in the lung is not clear. Here we propose that fueled by maternal exposure to DEP, NK cells become critically engaged in responses to inhaled allergens. By controlling production of type-2 mediators by the airway epithelium, NK cells contribute to induction of pulmonary type-2 responses and AAD.

Importance of NK cells in mouse models of AAD was explored in previous studies but the results were conflicting (47-49). One potential reason for lack of clarity was the use of non-specific tools for NK cell depletion. To address this, we used the *Ncr1*^{iCre}*R26*^{DTA} strain of mice, representing the most specific model of NK cell deficiency to date. We then complemented these studies through the use of NK cell-depleting antibodies anti-asialo-GM1 (this manuscript) and anti-NK1.1 (14), and by performing the NK cell reconstitution experiment. All experiments led to the same conclusion - NK cells drove AAD in our DEP-dependent model. We also observed that NK cells were redundant in models that rely exclusively on allergens to elicit AAD. This is consistent with a recent publication that used *Ncr1*^{iCre}*R26*^{DTA} mice to report no role of NK cells in adult allergen-driven AAD (22).

NK cell priming in our model may have several causes that likely act in concert. The first likely cause is cellular stress and cell damage that are triggered by transplacentally-transferred DEP and DEP-derived compounds or by endogenous molecules, including cytokines that are overproduced by DEP-challenged mothers and fetuses. Prior data provide a rationale to hypothesize that DEP activity extends beyond the exposure period (pre-conception) and into the pregnancy. DEP and DEP-derived polycyclic aromatic hydrocarbons (PAH) have been shown to persist in the body long after cessation of the exposure (50). PAH are known to cross the placental barrier (51). DEP are likely to have this capacity; a large proportion of DEPs are nanoparticles (52) and nanoparticles, in general, are easily transferrable via the placenta (53). Transplacentally-transferred DEP, PAH and DEP/PAH-induced endogenous molecules may stress or damage offspring cells. Stressed and damaged cells are known to activate NK cells through upregulation of NKG2D and DNAM-1 ligands, downregulation of MHCI and production of NK cell-stimulatory cytokines. Some of these molecules are linked to type-2 immunity. A previous study shows that physical damage of the epidermis (tape-stripping) results in upregulation of NKG2D ligands on keratinocytes (54). Under these circumstances, epidermal NKG2D ligands promote type-2 cytokine production by NKG2D-expressing intraepithelial lymphocytes; if skin damage is followed by allergen application to the damaged area, NKG2D^{+} type-2 cytokine-expressing lymphocytes initiate the type-2 immune response to this allergen, leading to induction of allergen-specific IgE. NK cells may

also be primed by DEP-derived compounds. NK cells express aryl hydrocarbon receptor (AHR), an environment-sensing transcriptional factor that is targeted by DEP-derived PAH. AHR promotes NK cell survival (55) and cytolytic activity (56). In other cell types, such as mast cells and T cells, PAH and AHR induce type-2 cytokines (57), suggesting that type-2 programming of NK cells in our model may be a result of AHR activation. We have evidence that the AHR pathway is activated in DEP-exposed mothers and their offspring (13, 14).

Lastly, we would like to comment on some of our results on ILC2s/Th2s. When comparing our data on IL-25 with data on IL-25 targets ($IL25R^+$ ILC2s/Th2s), we noticed an interesting discrepancy: DEP-PBS pups had moderately increased frequencies of these cells despite having normal levels of IL-25 (Figure 1E, H, J, Figure 4A and B). We speculate that moderate expansion of DEP-PBS $IL25R^+$ ILC2s and Th2 cells may be due to increased responsiveness of these cells to IL-25. Alternatively, this may be due to another DEP-regulated mediator that specifically targets $IL25R^+$ ILC2s and Th2 cells. We will address these hypotheses in another study.

Taken together, our studies provide proof-of-concept that the NK cell-airway epithelium axis plays an important role in DEP-triggered transmission of asthma predisposition from the mother to her offspring. We hope that the identified principles will facilitate development of new diagnostic tools for early detection and precise classification of asthma.

Methods

Additional information can be found in the Supplemental Methods.

Statistics

To compare the means of two matched groups and the means of two unmatched groups, 2-tailed paired and unpaired Student's t tests were used, respectively. To compare the means of three or more unmatched groups, the 1-way ANOVA test was performed, followed by Tukey's or Dunnett's post-hoc tests. To analyze data with 2 or more groups and repeated measurements on individual mice (FlexiVent studies), 2-way repeated measures ANOVA was used, followed by the Bonferroni post-hoc test. Data are presented as mean ± standard error of the mean (SEM). Statistical significance was defined as $P<0.05$. 'n' represented number of biological replicates and was defined in the figure legends. For box plots, lines within the boxes represent medians; boxes represent 25th-75th percentiles; and whiskers represent minimum and maximum values. All statistical analysis was performed using the Prism software (GraphPad 7).

Study approval

All procedures on animals were reviewed and approved by the Institutional Animal Care and Use Committee (IACUC) at National Jewish Health (NJH), Denver, CO (IACUC # AS2798-12-20). All studies on human samples were reviewed and approved by the Institutional Review Board (IRB) at NJH, Denver, CO (IRB # HS-3509 for the cord blood study and IRB # HS-2604 and HS-3114 for collection of bronchial brushings). Cord blood samples were received from the University of Colorado Cord Blood Bank, Aurora, CO. Bronchial brushings were collected during bronchoscopy by the NJH Biobank Honest Broker System, Denver CO. Brushings were then transferred to the Human Primary Cell Culture Core at National Jewish Health, Denver, CO, from which the samples were distributed to the study investigators. Prior to subject enrollment and sample collection, written informed consents were obtained from all subjects. Investigators in this study were not involved in subject enrollment, consenting and sample collection, and were blinded to donor identities.

Author contributions

Q.Q., B.P.C., Z.S. and J.L. performed experiments and analyzed data; M.M.G. conceived and directed the study, designed experiments and analyzed data; M.M.G. and Q.Q. prepared figures and wrote the manuscript; R.A. provided helpful discussion and reviewed the manuscript; E.V. generated a key mouse strain (*Ncr1*$^{iCre/+}$) and reviewed the manuscript.

Acknowledgments

This work was supported by NIH grant R01HL122995 and ALA Biomedical Research Grant RG-310463, both to M.M.G. E.V. generated *Ncr1*$^{iCre/+}$ mice and is supported by funding from the European Research Council (ERC) under the European Union's Horizon 2020 research and innovation program (TILC, grant agreement N°694502); the Agence Nationale de la Recherche; Equipe Labellisée "La Ligue," Ligue Nationale contre le Cancer, MSDAvenir, Innate Pharma and institutional grants to the CIML (INSERM, CNRS, and Aix-Marseille University) and to Marseille Immunopôle. We thank Dr. Joseph Sun (Memorial Sloan Kettering Cancer Center, New York, NY, USA) for sending *Ncr1*$^{iCre/+}$ mice, Drs. Timothy J. Ley (Washington University School of Medicine, St. Louis, MO, USA) and Xuefang Cao (Roswell Park Comprehensive Cancer Center, Buffalo, NY, USA) for generating and sending *Gzmb*$^{-/-}$ mice, respectively.

References

1. Bisgaard H, Bønnelykke K. Long-term studies of the natural history of asthma in childhood. *J Allergy Clin Immunol.* 2010;126:187-197.
2. Vercelli D. Does epigenetics play a role in human asthma? *Allergol Int.* 2016;65(2):123-126.
3. Igartua C, et al. Ethnic-specific associations of rare and low-frequency DNA sequence variants with asthma. *Nat Commun.* 2015;6:5965.
4. von Mutius E, Martinez FD, Fritzsch C, Nicolai T, Roell G, Thiemann HH. Prevalence of asthma and atopy in two areas of West and East Germany. *Am J Respir Crit Care Med.* 1994;149(2 Pt 1):358-364.
5. Riedler J, Eder W, Oberfeld G, Schreuer M. Austrian children living on a farm have less hay fever, asthma and allergic sensitization. *Clin Exp Allergy*. 2000;30(2):194-200.
6. Brandt EB, Myers JM, Ryan PH, Hershey GK. Air pollution and allergic diseases. *Curr Opin Pediatr*. 2015;27(6):724-735.
7. Illi S, et al. Protection from childhood asthma and allergy in Alpine farm environments-the GABRIEL Advanced Studies. *J Allergy Clin Immunol*. 2012;129(6):1470-1477.
8. McConnell R, et al. Childhood incident asthma and traffic-related air pollution at home and school. *Environ Health Perspect*. 2010;118(7):1021-1026.
9. Ryan PH, et al. Is it traffic type, volume, or distance? Wheezing in infants living near truck and bus traffic. *J Allergy Clin Immunol.* 2005;116(2):279-284.
10. Muranaka M, et al. Adjuvant activity of diesel-exhaust particulates for the production of IgE antibody in mice. *J Allergy Clin Immunol.* 1986;77(4):616-623.
11. Hsu HH, et al. Prenatal Particulate Air Pollution and Asthma Onset in Urban Children. Identifying Sensitive Windows and Sex Difference. *Am J Respir Crit Care Med.* 2015;192(9):1052-1059.
12. Jedrychowski WA, et al. Intrauterine exposure to polycyclic aromatic hydrocarbons, fine particulate matter and early wheeze. Prospective birth cohort study in 4-year olds. *Pediatr Allergy Immunol*. 2010;21(4 Pt 2):e723-732.

13. Lenberg J, Qian Q, Sun Z, Alam R, Gorska MM. Pre-pregnancy exposure to diesel exhaust predisposes offspring to asthma through IL-1β and IL-17A. *J Allergy Clin Immunol*. 2018;141(3):1118-1122.

14. Manners S, Alam R, Schwartz DA, Gorska MM. A mouse model links asthma susceptibility to prenatal exposure to diesel exhaust. *J Allergy Clin Immunol*. 2014;134(1):63-72.

15. Chiossone L, Chaix J, Fuseri N, Roth C, Vivier E, Walzer T. Maturation of mouse NK cells is a 4-stage developmental program. *Blood* 2009;113(22):5488-5496.

16. Sun JC, Beilke JN, Lanier LL. Adaptive immune features of natural killer cells. *Nature* 2009;457(7229):557-561.

17. Narni-Mancinelli E, et al. Fate mapping analysis of lymphoid cells expressing the NKp46 cell surface receptor. *Proc Natl Acad Sci U S A.* 2011;108(45):18324-18329.

18. Bezman NA, et al. Immunological Genome Project Consortium. Molecular definition of the identity and activation of natural killer cells. *Nat Immunol*. 2012;13(10):1000-1009.

19. Rankin LC, et al. Complementarity and redundancy of IL-22-producing innate lymphoid cells. *Nat Immunol*. 2016;17(2):179-186.

20. Matsumoto A, et al. IL-22-producing RORγt-dependent innate lymphoid cells play a novel protective role in murine acute hepatitis. *PLoS One* 2013;8(4):e62853.

21. Vonarbourg C, et al. Regulated expression of nuclear receptor RORγt confers distinct functional fates to NK cell receptor-expressing RORγt(+) innate lymphocytes. *Immunity.* 2010;33(5):736-751.

22. Haspeslagh E, et al. Role of NKp46(+) natural killer cells in house dust mite-driven asthma. *EMBO Mol Med*. 2018;10(4):e8657.Zhao A, et al. Critical role of IL-25 in nematode infection-induced alterations in intestinal function. *J Immunol*. 2010;185(11):6921-6929.

23. Hanna J, Bechtel P, Zhai Y, Youssef F, McLachlan K, Mandelboim O. Novel insights on human NK cells' immunological modalities revealed by gene expression profiling. *J Immunol*. 2004;173(11):6547-6563.

24. Voskoboinik I, Whisstock JC, Trapani JA. Perforin and granzymes: function, dysfunction and human pathology. *Nat Rev Immunol*. 2015;15(6):388-400.

25. Froelich CJ, et al. New paradigm for lymphocyte granule-mediated cytotoxicity. Target cells bind and internalize granzyme B, but an endosomolytic agent is necessary for cytosolic delivery and subsequent apoptosis. *J Biol Chem*. 1996;271(46):29073-29079.

26. Molofsky AB, Savage AK, Locksley RM. Interleukin-33 in Tissue Homeostasis, Injury, and Inflammation. *Immunity.* 2015;42(6):1005-19.

27. Gerbe F, et al. Intestinal epithelial tuft cells initiate type 2 mucosal immunity to helminth parasites. *Nature.* 2016;529(7585):226-230.

28. Howitt MR, et al. Tuft cells, taste-chemosensory cells, orchestrate parasite type 2 immunity in the gut. *Science.* 2016;351(6279):1329-1333.

29. von Moltke J, Ji M, Liang HE, Locksley RM. Tuft-cell-derived IL-25 regulates an intestinal ILC2-epithelial response circuit. *Nature.* 2016;529(7585):221-225.

30. Kakkar R, Hei H, Dobner S, Lee RT. Interleukin 33 as a mechanically responsive cytokine secreted by living cells. *J Biol Chem*. 2012;287(9):6941-6948.

31. Kouzaki H, Iijima K, Kobayashi T, O'Grady SM, Kita H. The danger signal, extracellular ATP, is a sensor for an airborne allergen and triggers IL-33 release and innate Th2-type responses. *J Immunol*. 2011;186(7):4375-4387.

32. Altman MC, et al. Allergen-induced activation of natural killer cells represents an early-life immune response in the development of allergic asthma. *J Allergy Clin Immunol*. 2018;142(6):1856-1866.

33. Yang IV, et al. DNA methylation and childhood asthma in the inner city. *J Allergy Clin Immunol.* 2015;136(1):69-80

34. Hong JY, et al. Neonatal rhinovirus induces mucous metaplasia and airways hyperresponsiveness through IL-25 and type 2 innate lymphoid cells. *J Allergy Clin Immunol.* 2014;134(2):429-439.

35. Sadeghnejad A, Karmaus W, Davis S, Kurukulaaratchy RJ, Matthews S, Arshad SH. Raised cord serum immunoglobulin E increases the risk of allergic sensitization at ages 4 and 10 and asthma at age 10. *Thorax.* 2004;59(11):936-942.

36. Piccioli D, Sbrana S, Melandri E, Valiante NM. Contact-dependent stimulation and inhibition of dendritic cells by natural killer cells. *J Exp Med*. 2002;195(3):335-341.

37. Wei H, Zhang J, Xiao W, Feng J, Sun R, Tian Z. Involvement of human natural killer cells in asthma pathogenesis: natural killer 2 cells in type 2 cytokine predominance. *J Allergy Clin Immunol.* 2005;115(4):841-847.

38. Barnig C, et al. Lipoxin A4 regulates natural killer cell and type 2 innate lymphoid cell activation in asthma. *Sci Transl Med*. 2013;5(174):174ra26.

39. Prakash MD, et al. Granzyme B promotes cytotoxic lymphocyte transmigration via basement membrane remodeling. *Immunity.* 2014;41(6):960-972.

40. Wensink AC, et al. Granzyme K synergistically potentiates LPS-induced cytokine responses in human monocytes. *Proc Natl Acad Sci U S A*. 2014;111(16):5974-5979.

41. Afonina IS, et al. Granzyme B-dependent proteolysis acts as a switch to enhance the proinflammatory activity of IL-1α. *Mol Cell.* 2011;44(2):265-278.

42. Asokananthan N, et al. House dust mite allergens induce proinflammatory cytokines from respiratory epithelial cells: the cysteine protease allergen, Der p 1, activates protease-activated receptor (PAR)-2 and inactivates PAR-1. *J Immunol*. 2002;169(8):4572-4578.

43. Grégoire C, et al. The trafficking of natural killer cells. *Immunol Rev*. 2007;220:169-182.

44. Zhou G, Juang SW, Kane KP. NK cells exacerbate the pathology of influenza virus infection in mice. *Eur J Immunol*. 2013;43(4):929-938.

45. Motz GT, et al. Chronic cigarette smoke exposure primes NK cells activation in a mouse model of chronic obstructive pulmonary disease. *J Immunol*. 2010;184(8):4460-4469.

46. Haworth O, Cernadas M, Levy BD. NK cells are effectors for resolvin E1 in the timely resolution of allergic airway inflammation. *J Immunol*. 2011;186(11):6129-6135.

47. Korsgren M, et al. Natural killer cells determine development of allergen-induced eosinophilic airway inflammation in mice. *J Exp Med*. 1999;189(3):553-562.

48. Mathias CB, et al. Pro-inflammatory role of natural killer cells in the development of allergic airway disease. *Clin Exp Allergy.* 2014;44(4):589-601.

49. Gerde P, Muggenburg BA, Lundborg M, Dahl AR. The rapid alveolar absorption of diesel soot-adsorbed benzo[a]pyrene: bioavailability, metabolism and dosimetry of an inhaled particle-borne carcinogen. *Carcinogenesis.* 2001;22(5):741-749.

50. Srivastava VK, Chauhan SS, Srivastava PK, Kumar V, Misra UK. Fetal translocation and metabolism of PAH obtained from coal fly ash given intratracheally to pregnant rats. *J Toxicol Environ Health*. 1986;18(3):459-469.

51. Li N, et al. A work group report on ultrafine particles (American Academy of Allergy, Asthma & Immunology): Why ambient ultrafine and engineered nanoparticles should receive special attention for possible adverse health outcomes in human subjects. *J Allergy Clin Immunol.* 2016;138(2):386-96.

52. Wick P, et al. Barrier capacity of human placenta for nanosized materials. *Environ Health Perspect.* 2010;118(3):432-6.

53. Strid J, Sobolev O, Zafirova B, Polic B, Hayday A. The intraepithelial T cell response to NKG2D-ligands links lymphoid stress surveillance to atopy. *Science.* 2011;334(6060):1293-7.

54. Zhang LH, Shin JH, Haggadone MD, Sunwoo JB. The aryl hydrocarbon receptor is required for the maintenance of liver-resident natural killer cells. *J Exp Med.* 2016;213(11):2249-2257.

55. Shin JH, et al. Modulation of natural killer cell antitumor activity by the aryl hydrocarbon receptor. *Proc Natl Acad Sci U S A*. 2013;110(30):12391-6.

56. Bömmel H, Li-Weber M, Serfling E, Duschl A. The environmental pollutant pyrene induces the production of IL-4. *J Allergy Clin Immunol.* 2000;105(4):796-802.

Figures and figure legends

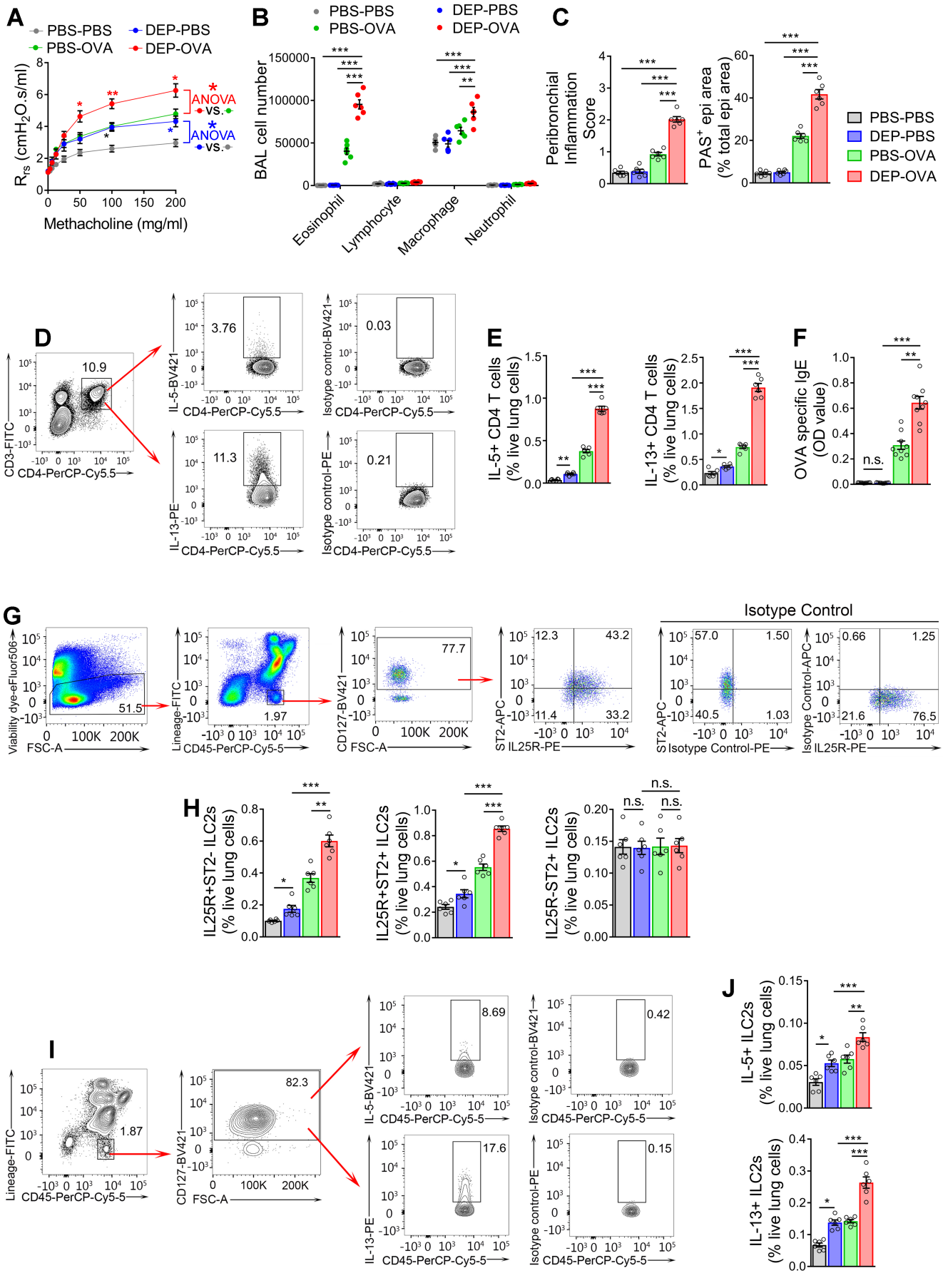

Figure 1. Maternal exposure to DEP enhances the type-2 immune response and AAD in offspring.

(A-J) AAD and the type-2 immune response in the lungs of PBS-PBS, DEP-PBS, PBS-OVA and DEP-OVA pups. **(A)** Total lung resistance to methacholine (FlexiVent). n=6 pups per group**. (B**) Leukocyte subsets in the bronchoalveolar lavage (BAL) fluid. n=6. **(C)** Peribronchial inflammation scores (left) and proportions of bronchial epithelial (epi) areas that are PAS (mucin)+ (right). n=6. (**D**) Flow cytometry (FC) plots to quantify pulmonary IL-5$^+$ and IL-13$^+$ CD4 T cells. PMA/ionomycin-stimulated lung cell suspensions were stained for flow cytometry. After exclusion of debris, doublets and dead cells, live (eFluor506$^-$) singlets were analyzed for CD3 and CD4. CD3$^+$CD4$^+$ cells were analyzed for IL-5 and IL-13. **(E**) Percentages of cytokine$^+$ CD4 T cells in live lung cells**.** n=6. **(F)** OVA-specific IgE in the serum. n=9**. (G**) FC plots to quantify lung ILC2 subsets. Live lung singlets (no ex vivo stimulation) were analyzed for Lineage/Lin markers (CD3, B220, CD11b, CD11c, Gr1, FcεRIα and NK1.1) and CD45. CD45$^+$Lin$^-$ cells were analyzed for CD127. CD127$^+$ cells were analyzed for IL25R and ST2 to quantify IL25R$^+$ST2$^-$, IL25R$^+$ST2$^+$ and IL25R$^-$ST2$^+$ ILC2 subsets (CD45$^+$Lin$^-$ CD127$^+$IL25R$^+$ST2$^-$, CD45$^+$Lin$^-$CD127$^+$IL25R$^+$ST2$^+$ and CD45$^+$Lin$^-$CD127$^+$IL25R$^-$ST2$^+$ cells, respectively). **(H**) Percentages of ILC2 subsets in live lung cells. n=6. (**I**) Gating strategy to quantify pulmonary IL-5$^+$ and IL-13$^+$ ILC2s. PMA/ionomycin-stimulated eFluor506$^-$ lung singlets were analyzed for CD45 and Lineage markers. CD45$^+$Lin$^-$ cells were analyzed for CD127. CD45$^+$Lin$^-$CD127$^+$ cells were analyzed for IL-5 and IL-13. **(J**) Percentages of cytokine$^+$ ILC2s in live lung cells. n=6. Data are representative of 3 independent experiments, and are shown as mean ± SEM. *$P < 0.05$, **$P < 0.01$, ***$P < 0.001$, by 2-way repeated measures ANOVA with Bonferroni post-hoc test (A) and 1-way ANOVA with Tukey's post-hoc test (B, C, E, F, H, J). n.s. not significant

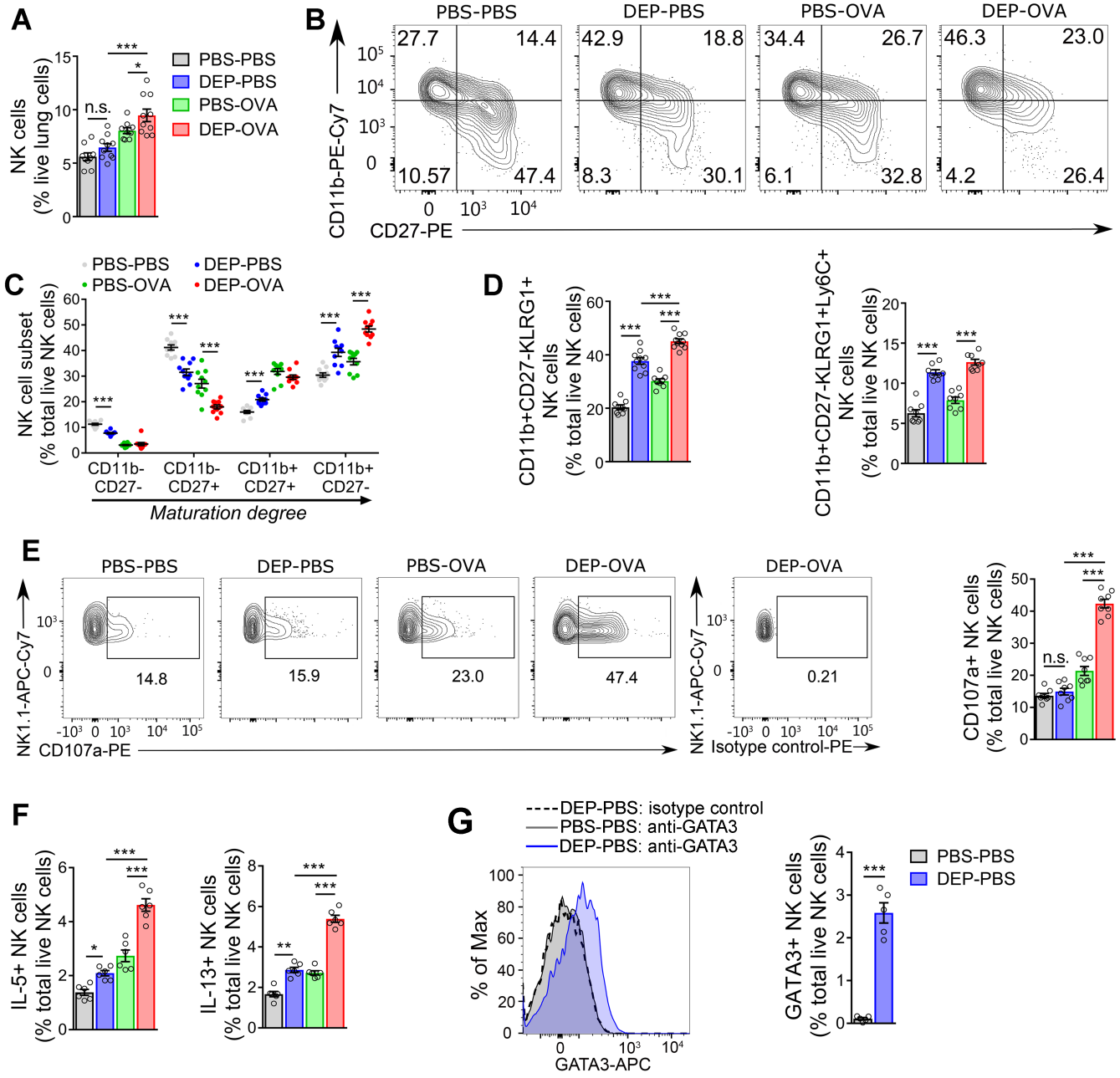

Figure 2. 'DEP' NK cells have increased capacity to produce type-2 cytokines and degranulate.

(A-G) Frequencies and features of lung NK cells in PBS-PBS, DEP-PBS, PBS-OVA and DEP-OVA pups. (**A**) Percentage of NK cells ($CD3^-CD19^-NK1.1^+$) in live lung cells. n=9-10 mice per group. (**B**) FC plots to detect NK cell subsets. $CD3^-CD19^-NK1.1^+$ live lung cells were analyzed for CD11b and CD27. (**C, D**) Percentages of indicated subsets in live lung NK cells. n=9-10 mice per group (B-D: gating strategy in Supplemental Figure 2A) (**E**) Left: FC plots to measure degranulated ($CD107a^+$) NK cells in lung digests. Lung cells were incubated at 37^0C with PE-labeled anti-CD107a or isotype control IgG, monensin, brefeldin A, IL-2 and IL-15, and then

stained with eFluor506 and antibodies for surface markers. Live NK cells (eFluor506$^-$CD3$^-$CD19$^-$NK1.1$^+$) were analyzed for NK1.1 vs. CD107a. Right: percentage of CD107a$^+$ NK cells in live lung NK cells. n=8. (**F**) Percentages of IL-5$^+$/IL-13$^+$ NK cells in live lung NK cells. The result was obtained after ex vivo stimulation with PMA/ionomycin. n=6. (**G**) Left: FC plot to identify GATA3$^+$ NK cells. CD3$^-$CD19$^-$CD127$^-$NK1.1$^+$ live lung cells (no ex vivo stimulation) from PBS-PBS and DEP-PBS pups were analyzed for GATA3 or binding of an isotype control immunoglobulin. Right: Percentages of GATA3$^+$ NK cells in live lung NK cells. n=5. Data are representative of 2 independent experiments and are shown as mean ± SEM. *$P < 0.05$, **$P < 0.01$, ***$P < 0.001$, by 1-way ANOVA with Tukey's post-hoc test (A, C-F) and 2-tailed unpaired t test (G). n.s. not significant

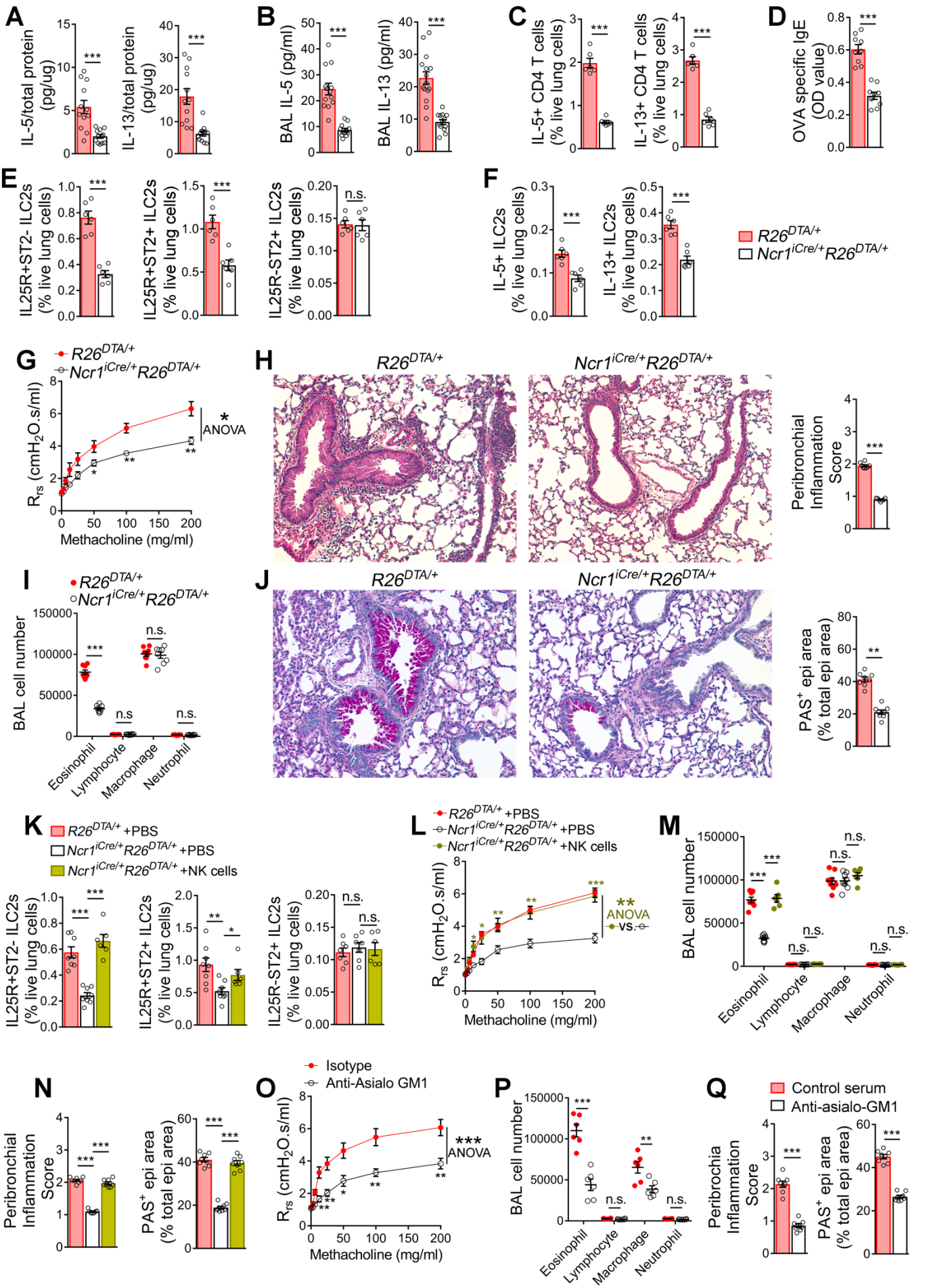
A
IL-5/total protein (pg/ug)
IL-13/total protein (pg/ug)
B
BAL IL-5 (pg/ml)
BAL IL-13 (pg/ml)
C
IL-5+ CD4 T cells (% live lung cells)
IL-13+ CD4 T cells (% live lung cells)
D
OVA specific IgE (OD value)
E
IL25R+ST2- ILC2s (% live lung cells)
IL25R+ST2+ ILC2s (% live lung cells)
IL25R-ST2+ ILC2s (% live lung cells)
n.s.
F
IL-5+ ILC2s (% live lung cells)
IL-13+ ILC2s (% live lung cells)
R26DTA/+
Ncr1iCre/+R26DTA/+
G
R26DTA/+
Ncr1iCre/+R26DTA/+
Rrs (cmH2O.s/ml)
Methacholine (mg/ml)
ANOVA
H
R26DTA/+
Ncr1iCre/+R26DTA/+
Peribronchial Inflammation Score
I
R26DTA/+
Ncr1iCre/+R26DTA/+
BAL cell number
n.s
Eosinophil
Lymphocyte
Macrophage
Neutrophil
J
R26DTA/+
Ncr1iCre/+R26DTA/+
PAS+ epi area (% total epi area)
K
R26DTA/+ +PBS
Ncr1iCre/+R26DTA/+ +PBS
Ncr1iCre/+R26DTA/+ +NK cells
IL25R+ST2- ILC2s (% live lung cells)
IL25R+ST2+ ILC2s (% live lung cells)
IL25R-ST2+ ILC2s (% live lung cells)
L
R26DTA/+ +PBS
Ncr1iCre/+R26DTA/+ +PBS
Ncr1iCre/+R26DTA/+ +NK cells
Rrs (cmH2O.s/ml)
Methacholine (mg/ml)
ANOVA
vs.
M
BAL cell number
Eosinophil
Lymphocyte
Macrophage
Neutrophil
N
Peribronchial Inflammation Score
PAS+ epi area (% total epi area)
O
Isotype
Anti-Asialo GM1
Rrs (cmH2O.s/ml)
Methacholine (mg/ml)
ANOVA
P
BAL cell number
Eosinophil
Lymphocyte
Macrophage
Neutrophil
Q
Control serum
Anti-asialo-GM1
Peribrochia Inflammation Score
PAS+ epi area (% total epi area)

Figure 3. The type-2 immune response and AAD are driven by NK cells.

(A-J) Genetic depletion of NK cells. DEP-exposed *Ncr1*$^{iCre/+}$ females were mated with unexposed *R26*$^{DTA/DTA}$ males to produce *Ncr1*$^{iCre/+}$*R26*$^{DTA/+}$ and *R26*$^{DTA/+}$ littermates. Pups were immunized and challenged with OVA, and analyzed 72 hours after challenge. (**K-N**) NK cell reconstitution. *Ncr1*$^{iCre/+}$*R26*$^{DTA/+}$ and *R26*$^{DTA/+}$ pups of DEP-exposed *Ncr1*$^{iCre/+}$ females were immunized with OVA on PND 5. On PND 22, a sub-group of *Ncr1*$^{iCre/+}$*R26*$^{DTA/+}$ pups was transferred with splenic CD127^{-} NK cells from *R26*$^{DTA/+}$ littermates. Other pups received PBS. NK cell/PBS recipients were challenged with OVA on PND 23-25 and analyzed on PND 28 (diagram of experimental strategy in Supplemental Figure 3B). **(O-Q**) Antibody-mediated depletion of NK cells. *Wt* DEP-OVA pups received anti-asialo-GM1 or control sera as in Supplemental Figure 3C. (**A, B**) IL-5 and IL-13 in lung homogenates (A, n=12) and the BAL fluid (B, n=13-15). **(C, E, F, K**) Cytokine^{+} CD4 T cells (C, n=6), IL25R^{+}ST2^{-}, IL25R^{+}ST2^{+} and IL25R^{-}ST2^{+} ILC2s (E, n=6; K, n=6-8) and cytokine^{+} ILC2s (F, n=6) in live lung cells**. (D)** OVA-specific IgE in serum. n=9. **(G, L, O**) Total lung resistance to methacholine. n=6 (G, L), n=5 (O). **(H, J, N, Q**) H&E and PAS stained lung sections (original magnification, x100), peribronchial inflammation scores and proportions of bronchial epithelial (epi) cell areas that are PAS+. n=7 (H), n=8 (J, N, Q). (**I, M, P**) Leukocyte subsets in the BAL fluid n=8 (I), n=6-8 (M) and n=6 (P)**.** Data are representative of two (A, B) or three (C-Q) independent experiments and are shown as mean ± SEM. **P* < 0.05, ***P* < 0.01, ****P* < 0.001, by 2-tailed unpaired t test (A-F, H-J, P, Q), 1-way ANOVA with Tukey's post-hoc test (K, M, N) and 2-way repeated measures ANOVA with Bonferroni post-hoc test (G, L, O).

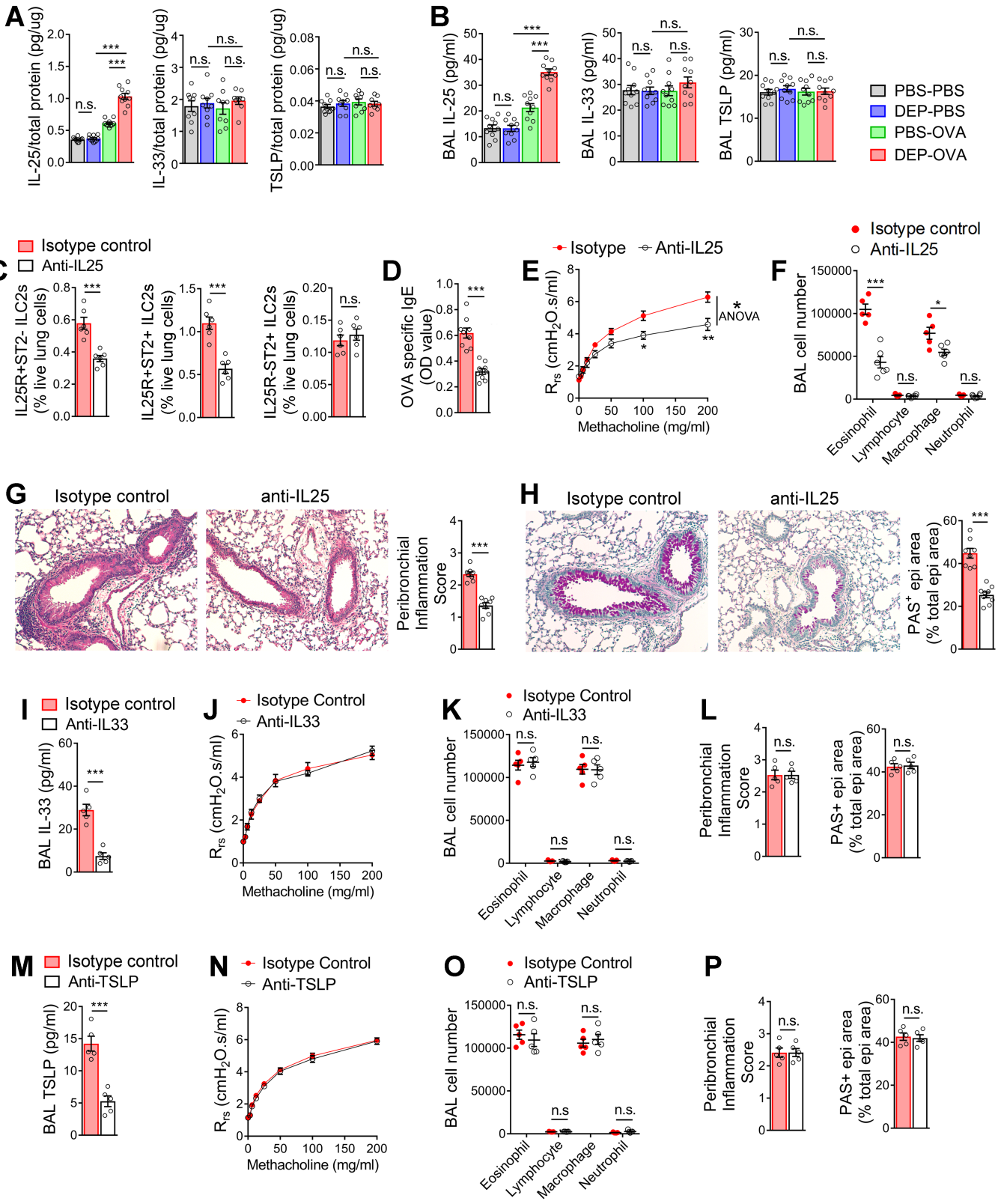

Figure 4. The type-2 immune response and AAD are dependent on IL-25.

(A, B) Concentrations of IL-25, IL-33, and TSLP in lung homogenates [A, n=10 (IL-25) or n=9 (IL-33, TSLP)] and the BAL fluid (B, n=10) from PBS-PBS, DEP-PBS, PBS-OVA and DEP-OVA pups. (**C-P**) Depletion of

IL-25 (C-H), IL-33 (I-L) and TSLP (M-P) in DEP-OVA pups. Pups received an anti-cytokine (anti-IL-25/anti-IL-33/anti-TSLP) antibody or isotype control IgG before immunization and then before the first challenge with OVA, and were analyzed 72 hours after the final challenge (diagram of experimental strategy in Supplemental Figure 4B). (**C**) Percentages of $IL25R^+ST2^-$ ILC2s, $IL25R^+ST2^+$ ILC2s and $IL25R^-ST2^+$ ILC2s in live lung cells. n=6. (**D**) OVA-specific IgE in the serum. n=9. (**E, J, N**) Total lung resistance to methacholine (FlexiVent). n=5-6. (**F, K, O**) Leukocyte subset counts in the BAL fluid. n=5-6. **(G, H, L, P**) Images of H&E-stained lung sections (original magnification, x100) (G), peribronchial inflammation scores (G, L, P), images of PAS-stained lung sections (original magnification, x100) (H) and proportions of bronchial epithelial (epi) areas that are PAS (mucin)+ (H, L, P). n=8-9 (anti-IL-25) and n=5 (anti-IL-33 and anti-TSLP). **(I, M)** Concentrations of IL-33 (I) and TSLP (M) in the BAL fluid. n=5. Data are representative of 2 (A, B, E, I-P) or 3 (C, D, F-H) independent experiments, and are shown as mean ± SEM. *$P < 0.05$, **$P < 0.01$, ***$P < 0.001$, by 1-way ANOVA with Tukey's post-hoc test (A, B), 2-tailed unpaired t test (C, D, F-I, K-M, O, P) and 2-way repeated measures ANOVA with Bonferroni post-hoc test (E, J, N). n.s. not significant

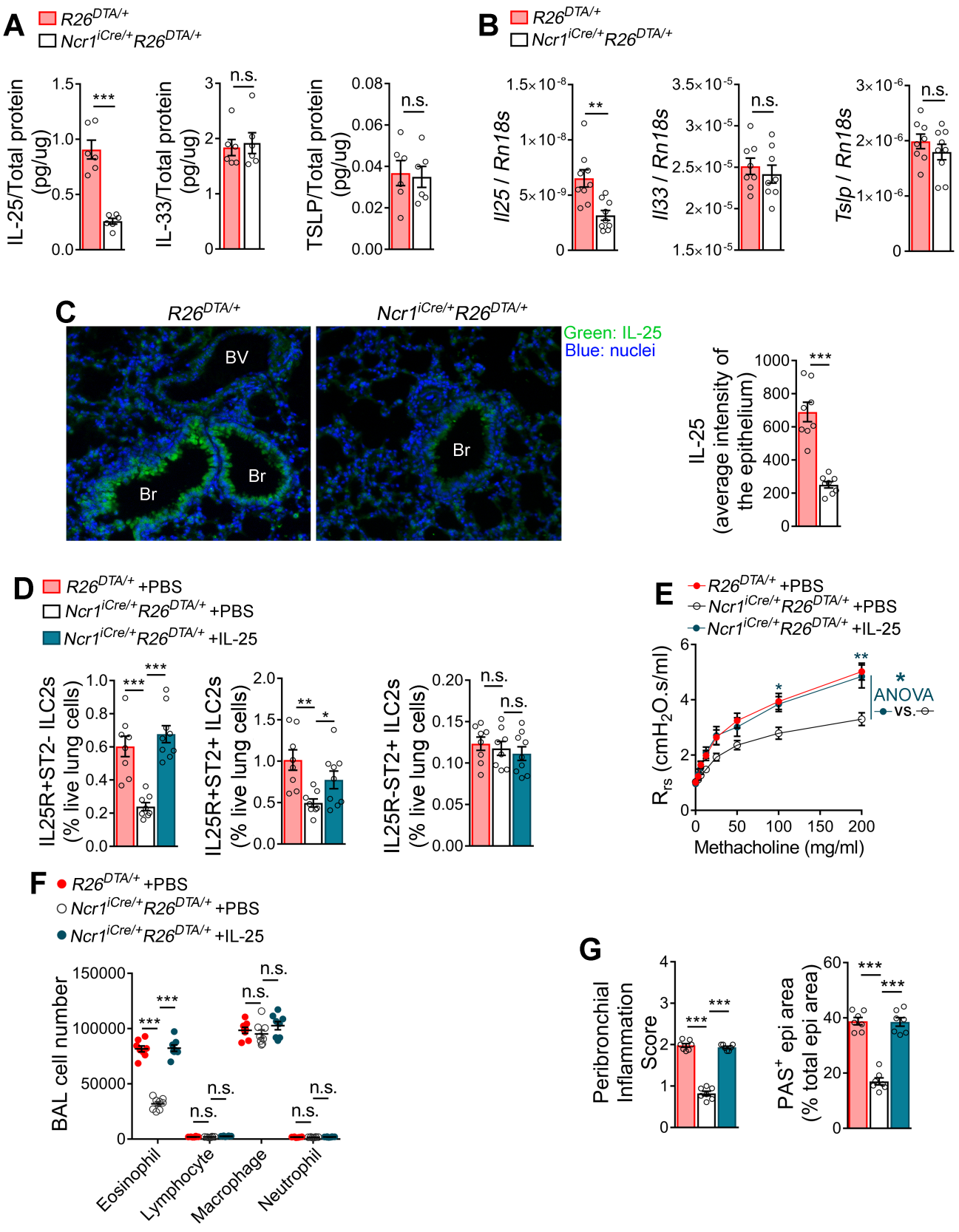

Figure 5. NK cells are upstream of IL-25.

(**A-C**) IL-25, IL-33, and TSLP in DEP-OVA *Ncr1*$^{iCre/+}$*R26*$^{DTA/+}$ and *R26*$^{DTA/+}$ littermates. (**A**) Concentrations of cytokines in lung homogenates. n=6 mice per group. (**B**) Levels of cytokine mRNAs in lung lysates; Rn18s,

18S ribosomal RNA. n=8-9. (**C**) Left: Fluorescent microscopy images of lung sections stained with an anti-IL-25 antibody (green) and the nuclear dye DAPI (blue); Br, bronchus, BV, blood vessel (original magnification, x200). Right: average fluorescence intensity of the IL-25 signal in the airway epithelium. n=8. (**D-G**) IL-25 reconstitution. Pups were produced as in Figure 3K-N. On postnatal day 5, pups were injected with OVA/alum mixed with IL-25 or PBS. IL-25/PBS injections were repeated on day 6 but this time no OVA/alum was used. All pups were OVA-challenged on days 23-25. Six hours after each challenge, pups were i.t. administered with IL-25 or PBS. Pups were analyzed on day 28 (diagram of experimental strategy in Supplemental Figure 5). (**D)** Percentages of $IL25R^{+}ST2^{-}$ ILC2s, $IL25R^{+}ST2^{+}$ ILC2s and $IL25R^{-}ST2^{+}$ ILC2s in live lung cells. n=8-9. (**E)** Total lung resistance to methacholine. n=7. (**F**) Leukocyte subset counts in the BAL fluid. n=8. (**G**) Peribronchial inflammation scores and proportions of bronchial epithelial (epi) areas that are PAS+. n=7. Data are representative of 3 independent experiments and are shown as mean ± SEM. $*P < 0.05$, $**P < 0.01$, $***P < 0.001$, by 2-tailed unpaired t test (A-C), 1-way ANOVA with Tukey's post-hoc test (D, F, G) and 2-way repeated measures ANOVA with Bonferroni post-hoc test (E). n.s. not significant

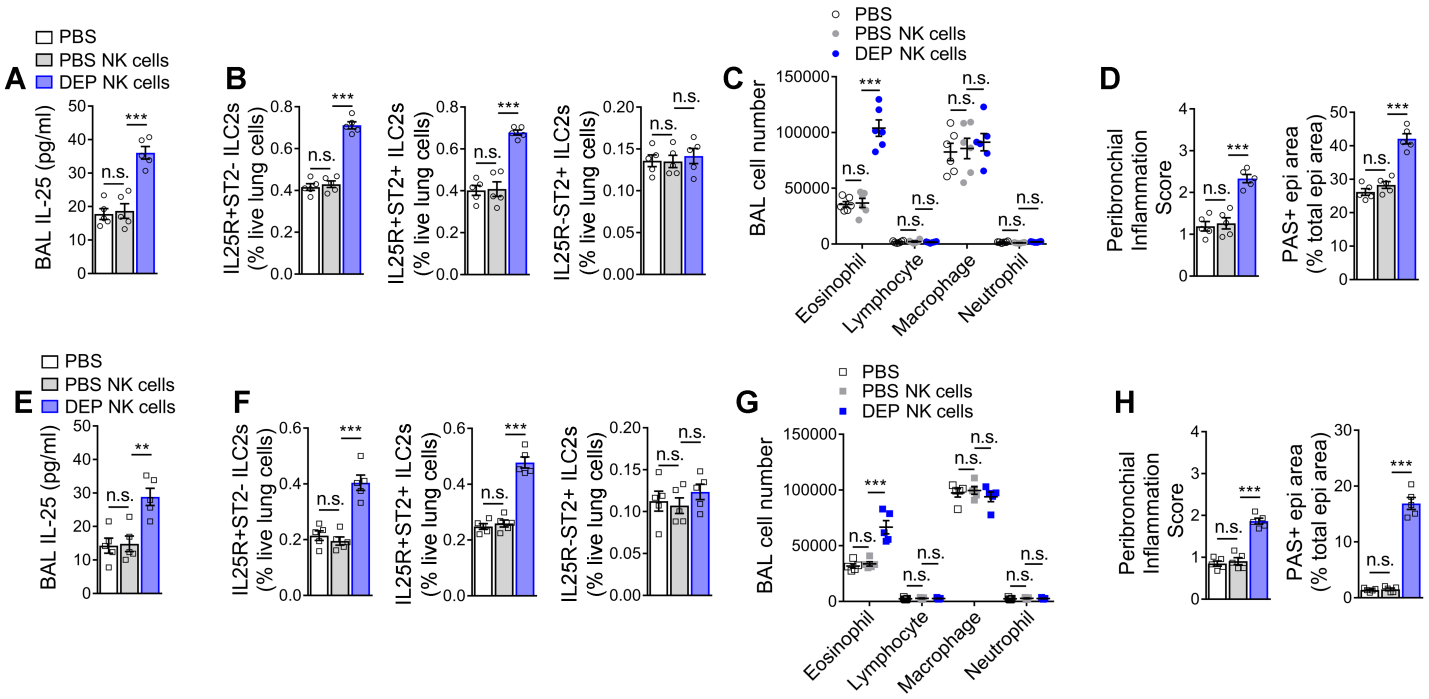

Figure 6. NK cells as carriers of susceptibility to AAD

(**A-H**) Transfer of NK cells from wild type pups of DEP-exposed and PBS-exposed mothers (DEP NK cells and PBS NK cells, respectively) into *Ncr1*$^{iCre/+}$*R26*$^{DTA/+}$ pups of unexposed mothers. Prospective recipient pups were immunized with OVA/alum on postnatal day 5 (protocol #1: Figure 6A-D) or postnatal day 26 (protocol #2: Figure 6E-H). Donor pups were not immunized. Transfer of CD127^{-} NK cells or PBS injection took place on day 22 (protocol #1) or day 43 (protocol #2), as in Figure 3K-N. Recipients were challenged with OVA on days 23-25 (protocol #1) or days 44-46 (protocol #2) and analyzed on day 28 (protocol #1) or day 49 (protocol #2) (diagram of experimental strategy in Supplemental Figure 6). (**A, E**) Concentration of IL-25 in the BAL fluid of recipients. (**B, F**) Percentages of IL25R^{+}ST2^{-} ILC2s, IL25R^{+}ST2^{+} ILC2s and IL25R^{-}ST2^{+} ILC2s in live lung cells of recipients. (**C, G**) Leukocyte subset counts in the BAL fluid of recipients. (**D, H**) Peribronchial inflammation scores and proportions of bronchial epithelial (epi) cell areas that are PAS+. A-H: n=6 (protocol #1), n=5 (protocol #2). Data are representative of 2 independent experiments and are shown as mean ± SEM. *$P < 0.05$, **$P < 0.01$, ***$P < 0.001$, by 1-way ANOVA with Tukey's post-hoc test. n.s. not significant

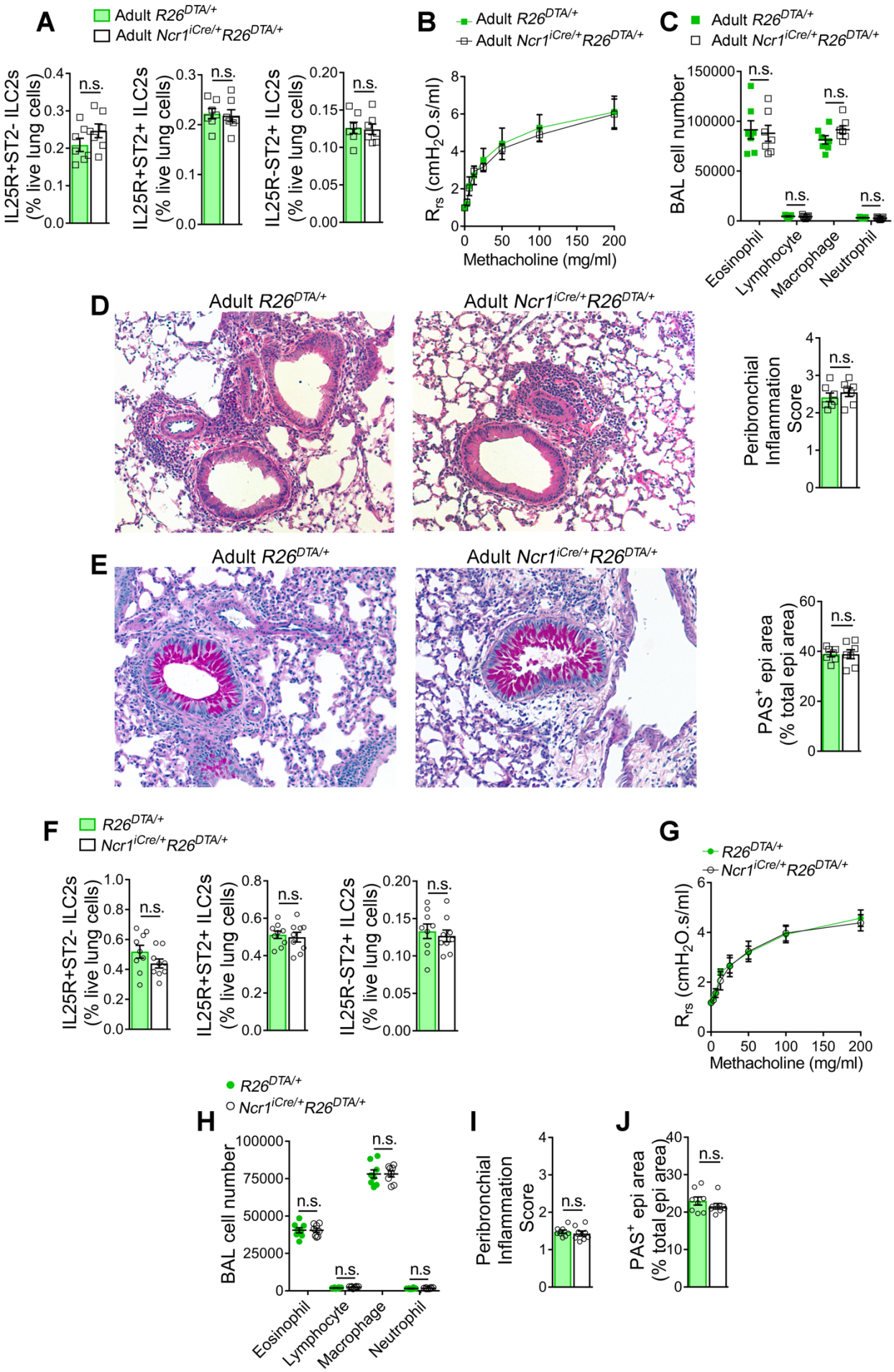
A
Adult R26DTA/+
Adult Ncr1iCre/+R26DTA/+
IL25R+ST2- ILC2s (% live lung cells)
IL25R+ST2+ ILC2s (% live lung cells)
IL25R-ST2+ ILC2s (% live lung cells)
n.s.
B
Adult R26DTA/+
Adult Ncr1iCre/+R26DTA/+
Rrs (cmH2O.s/ml)
Methacholine (mg/ml)
C
Adult R26DTA/+
Adult Ncr1iCre/+R26DTA/+
BAL cell number
Eosinophil
Lymphocyte
Macrophage
Neutrophil
D
Adult R26DTA/+
Adult Ncr1iCre/+R26DTA/+
Peribronchial Inflammation Score
E
Adult R26DTA/+
Adult Ncr1iCre/+R26DTA/+
PAS+ epi area (% total epi area)
F
R26DTA/+
Ncr1iCre/+R26DTA/+
IL25R+ST2- ILC2s (% live lung cells)
IL25R+ST2+ ILC2s (% live lung cells)
IL25R-ST2+ ILC2s (% live lung cells)
G
R26DTA/+
Ncr1iCre/+R26DTA/+
Rrs (cmH2O.s/ml)
Methacholine (mg/ml)
H
R26DTA/+
Ncr1iCre/+R26DTA/+
BAL cell number
Eosinophil
Lymphocyte
Macrophage
Neutrophil
I
Peribronchial Inflammation Score
J
PAS+ epi area (% total epi area)

Figure 7. NK cell engagement is unique to maternal DEP-programmed AAD.

(A-E) Adult mouse model of AAD. Unexposed *Ncr1*$^{iCre/+}$ females were mated with unexposed *R26*$^{DTA/DTA}$ males. *Ncr1*$^{iCre/+}$*R26*$^{DTA/+}$ and *R26*$^{DTA/+}$ offspring were i.p. immunized with OVA in alum on postnatal days 42 and 49, i.n. challenged with OVA on days 56, 57, and 58, and analyzed on day 61 (diagram of experimental strategy in Supplemental Figure 7). (**F-J**) Neonatal mouse model of AAD. PBS exposed *Ncr1*$^{iCre/+}$ females were mated with unexposed *R26*$^{DTA/DTA}$ males to produce *Ncr1*$^{iCre/+}$*R26*$^{DTA/+}$ and *R26*$^{DTA/+}$ littermates. Pups were immunized with OVA/alum on postnatal day 5, challenged with OVA on days 23-25, and analyzed on day 28. (**A, F**) Percentages of IL25R^{+}ST2^{-} ILC2s, IL25R^{+}ST2^{+} ILC2s and IL25R^{-}ST2^{+} ILC2s in live lung cells. n=7 mice per group (A) or n=9 (F). (**B, G**) Total lung resistance to methacholine. n=6 (B) and n=8 (G). (**C, H**) Leukocyte subset counts in the BAL fluid. n=7 (C) or n=8 (H). (**D**) Left: H&E-stained lung sections (original magnification, x100). Right: peribronchial inflammation scores. n=7. (**E**) Left: PAS-stained lung sections (original magnification, x100). Right: proportions of bronchial epithelial (epi) cell areas that are PAS+. n=7. (**I**) Peribronchial inflammation scores. n=8. (**J**) Proportions of bronchial epithelial (epi) areas that are PAS+. n=8. Data are representative of 3 (A-J) independent experiments and are shown as mean ± SEM. n.s. not significant, by 2-tailed unpaired t test (A, B, D-F, H-J) and 2-way repeated measures ANOVA with Bonferroni post-hoc test (C, G).

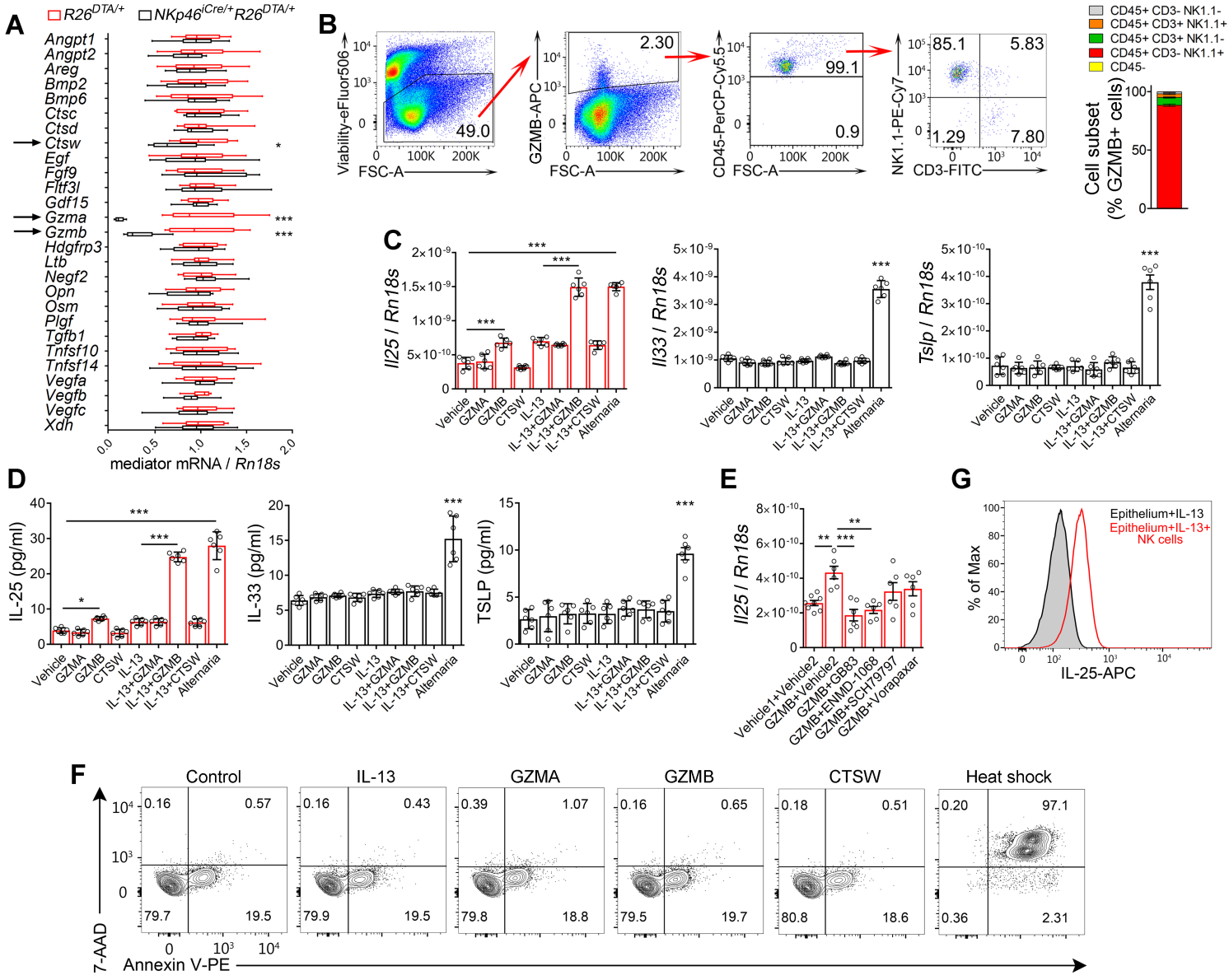

Figure 8. The NK cell granule protease granzyme B induces IL-25 in airway epithelial cells.

(A) Levels of mediator mRNAs in lungs of DEP-OVA *Ncr1*$^{iCre/+}$*R26*$^{DTA/+}$ and *R26*$^{DTA/+}$ littermates. n=10 mice per group. Lines within the boxes represent medians; boxes represent 25th-75th percentiles; and whiskers represent minimum and maximum values. (**B**) Left: Gating strategy to define lung cell subsets that express granzyme B (GZMB). Right: proportions of indicated cell subsets in the population of GZMB^{+} cells. n=7. (**C, D**) Production of *Il25*, *Il33* and *Tslp* mRNAs (C; cell lysates; n=6 samples per group) and IL-25, IL-33 and TSLP proteins (D; culture supernatants; n=6) by C57BL/6 Mouse Primary Tracheal and Bronchial Epithelial Cells (Cell Biologics, Inc.) treated with vehicle (PBS), granzyme A (GZMA), granzyme B (GZMB), cathepsin

W (CTSW) ± IL-13, or an extract of Alternaria alternata; Rn18s, 18S ribosomal RNA. (**E**) *Il25* mRNA in epithelial cells treated with GZMB, GZMB + PAR2 inhibitor (GB83 or ENMD-1068) and GZMB + PAR1 inhibitor (SCH79797 or Vorapaxar); vehicle 1 = PBS (vehicle for GZMB), vehicle 2 = DMSO (vehicle for inhibitors). n=8 (vehicle1+vehicle2) or n=6 (other conditions). (**F**) Flow cytometric (FC) detection of dead cells in cultures of epithelial cells treated as in Figure 8C, D or subjected to heat shock (positive control for cell death). (**G**) FC detection of IL-25 in $EpCAM^{+}NK1.1^{-}$ epithelial cells that were incubated with IL-13 ± NK cells from spleens of wild type DEP-OVA pups. Histogram is representative of 3 independent co-cultures. Data are representative of 2 (A, B) or 3 (C-G) independent experiments and are shown as mean ± SEM. $*P < 0.05$, $***P < 0.001$, by 2-tailed unpaired t test (A) and 1-way ANOVA with Tukey's post-hoc test (C-E).

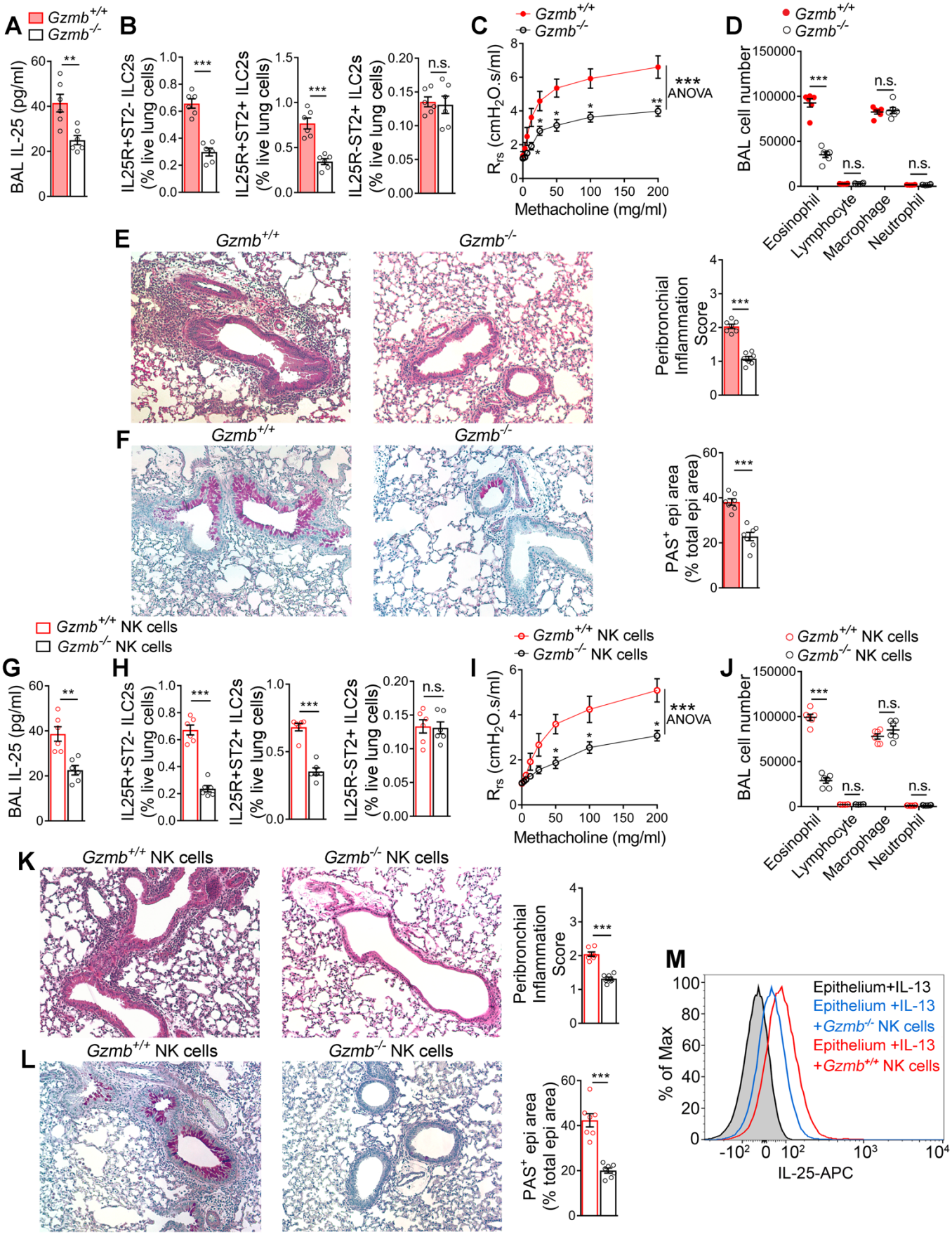
A
Gzmb+/+
Gzmb-/-
BAL IL-25 (pg/ml)
B
IL25R+ST2- ILC2s (% live lung cells)
IL25R+ST2+ ILC2s (% live lung cells)
IL25R-ST2+ ILC2s (% live lung cells)
n.s.
C
Rrs (cmH2O.s/ml)
Methacholine (mg/ml)
***
ANOVA
D
BAL cell number
Eosinophil
Lymphocyte
Macrophage
Neutrophil
E
Peribronchial Inflammation Score
F
PAS+ epi area (% total epi area)
Gzmb+/+ NK cells
Gzmb-/- NK cells
G
H
I
J
K
L
M
% of Max
IL-25-APC
Epithelium+IL-13
Epithelium +IL-13
+Gzmb-/- NK cells
Epithelium +IL-13
+Gzmb+/+ NK cells

Figure 9. Granzyme B is required for development of AAD in predisposed pups.

(A-F) Importance of systemic granzyme B. DEP exposed *Gzmb*$^{+/-}$ females were mated with unexposed *Gzmb*$^{+/-}$ males to generate *Gzmb*$^{-/-}$ and *Gzmb*$^{+/+}$ littermates. Pups were immunized, challenged with OVA and analyzed 72 hours after challenge. (**G-L**) Importance of NK cell-expressed granzyme B. *Ncr1*$^{iCre/+}$*R26*$^{DTA/+}$ pups were transferred with *Gzmb*$^{+/+}$ and *Gzmb*$^{-/-}$ NK cells. Donor and recipients had same age and were born to DEP exposed mothers. Cell transfer took place on day 22 as in Figure 3K-N. Before cell transfer, on postnatal day 5, donor and prospective recipient pups were immunized with OVA/alum. After cell transfer, recipients were challenged with OVA on days 23-25, and analyzed on day 28 (diagram of experimental strategy in Supplemental Figure 9). (**A, G**) Concentration of IL-25 in the BAL fluid. n=6 mice per group. (**B, H)** Percentages of IL25R^{+}ST2^{-} ILC2s, IL25R^{+}ST2^{+} ILC2s and IL25R^{-}ST2^{+} ILC2s in live lung cells. n=6. (**C, I**) Total lung resistance to methacholine. n=6. (**D, J**) Leukocyte subset counts in the BAL fluid. n=6. (**E, K**) Left: H&E-stained lung sections (original magnification, x100). Right: peribronchial inflammation scores. n=7. (**F, L**) Left: PAS-stained lung sections (original magnification, x100). Right: proportions of bronchial epithelial (epi) cell areas that are PAS+. n=7. (**M**) Flow cytometric detection of IL-25 in EpCAM^{+}NK1.1^{-} airway epithelial cells that were incubated with IL-13 ± NK cells from spleens of DEP-OVA *Gzmb*$^{+/+}$ and *Gzmb*$^{-/-}$ pups. Histogram is representative of 3 independent co-cultures. Data are representative of 3 independent experiments and are shown as mean ± SEM. **P* < 0.05, ****P* < 0.001, by 2-tailed unpaired t test (A, B, D-H, J-L) and 2-way repeated measures ANOVA with Bonferroni post-hoc test (C, I).

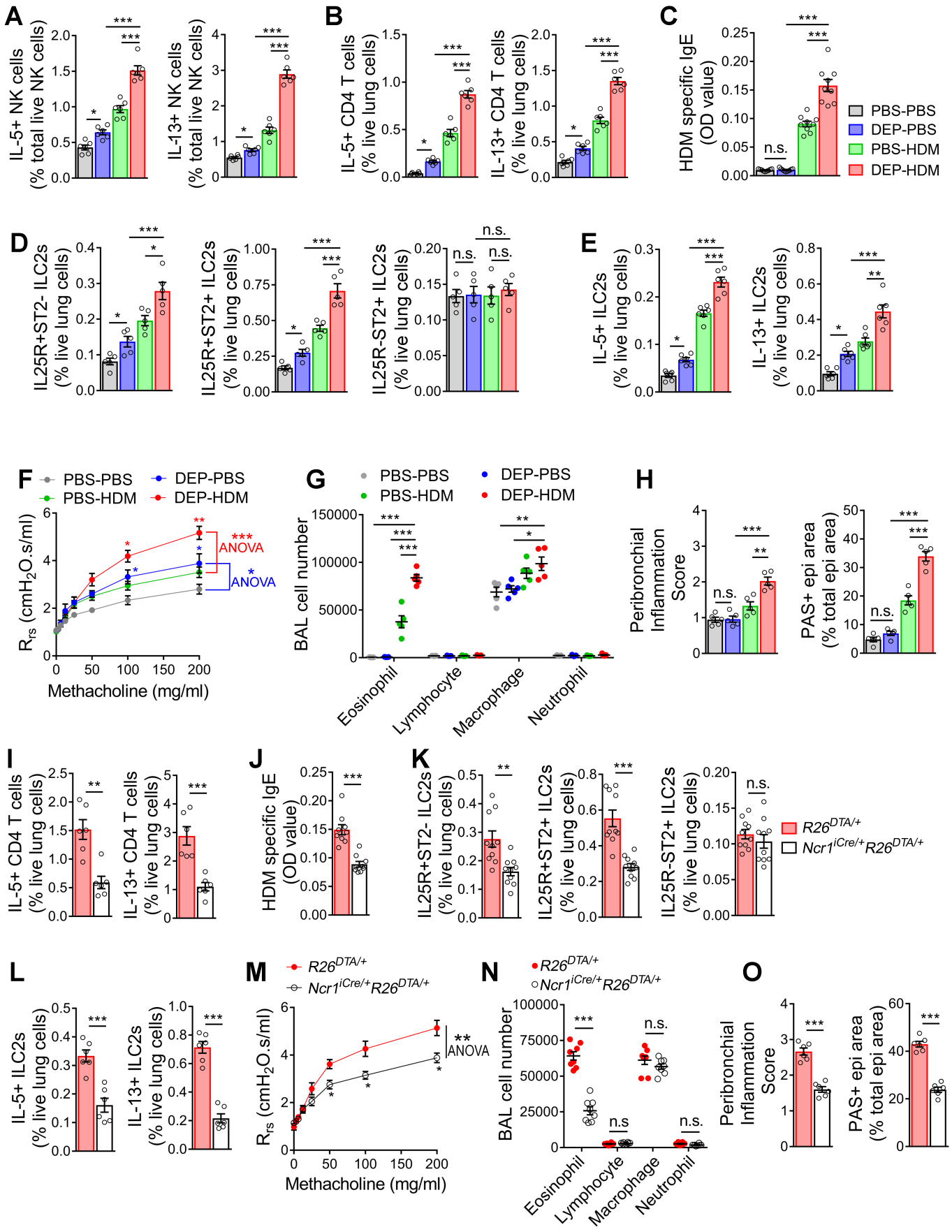
A
IL-5+ NK cells (% total live NK cells)
IL-13+ NK cells (% total live NK cells)
B
IL-5+ CD4 T cells (% live lung cells)
IL-13+ CD4 T cells (% live lung cells)
C
HDM specific IgE (OD value)
n.s.
PBS-PBS
DEP-PBS
PBS-HDM
DEP-HDM
D
IL25R+ST2- ILC2s (% live lung cells)
IL25R+ST2+ ILC2s (% live lung cells)
IL25R-ST2+ ILC2s (% live lung cells)
E
IL-5+ ILC2s (% live lung cells)
IL-13+ ILC2s (% live lung cells)
F
PBS-PBS
DEP-PBS
PBS-HDM
DEP-HDM
ANOVA
ANOVA
Rrs (cmH2O.s/ml)
Methacholine (mg/ml)
G
PBS-PBS
DEP-PBS
PBS-HDM
DEP-HDM
BAL cell number
Eosinophil
Lymphocyte
Macrophage
Neutrophil
H
Peribronchial Inflammation Score
PAS+ epi area (% total epi area)
I
IL-5+ CD4 T cells (% live lung cells)
IL-13+ CD4 T cells (% live lung cells)
J
HDM specific IgE (OD value)
K
IL25R+ST2- ILC2s (% live lung cells)
IL25R+ST2+ ILC2s (% live lung cells)
IL25R-ST2+ ILC2s (% live lung cells)
R26DTA/+
Ncr1iCre/+R26DTA/+
L
IL-5+ ILC2s (% live lung cells)
IL-13+ ILC2s (% live lung cells)
M
R26DTA/+
Ncr1iCre/+R26DTA/+
ANOVA
Rrs (cmH2O.s/ml)
Methacholine (mg/ml)
N
R26DTA/+
Ncr1iCre/+R26DTA/+
BAL cell number
Eosinophil
Lymphocyte
Macrophage
Neutrophil
O
Peribronchial Inflammation Score
PAS+ epi area (% total epi area)

Figure 10. 'DEP' NK cells drive AAD to HDM

(**A-H**) Model of early-life AAD to HDM in the context of maternal exposure to DEP. Pups of DEP-exposed and PBS-exposed mothers received HDM intranasally on postnatal days 5 and 6 (immunization phase) and then on postnatal days 23, 24 and 25 (challenge phase). Pups were analyzed on postnatal day 28 (diagram of experimental strategy in Supplemental Figure 10). (**I-O**) Genetic depletion of NK cells in DEP-HDM pups. 'DEP' *Ncr1*$^{iCre/+}$*R26*$^{DTA/+}$ and *R26*$^{DTA/+}$ littermate pups were generated as in Figure 3A-J. After birth, pups were immunized and challenged with HDM, and analyzed 72 hours after challenge. (**A**) Percentages of IL-5$^+$ and IL-13$^+$ NK cells in live lung NK cells (after ex vivo stimulation with PMA/ionomycin). n=6 per group. (**B, I**) Percentages of IL-5$^+$ and IL-13$^+$ CD4 T cells in live lung cells. n=6. (**C, J**) HDM-specific IgE in the serum. n=9. (**D, K**) Percentages of IL25R$^+$ST2$^-$ ILC2s, IL25R$^+$ST2$^+$ ILC2s and IL25R$^-$ST2$^+$ ILC2s in live lung cells. n=5 (D) and n=10 (K). (**E, L**) Percentages of IL-5$^+$ and IL-13$^+$ ILC2s in live lung cells. n=6. (**F, M**) Total lung resistance to methacholine. n=6**. (G, N)** Leukocyte subset counts in the BAL fluid. n=5 (G) and n=8 (N). (**H, O**) Peribronchial inflammation scores (left, n=5) and proportions of bronchial epithelial (epi) areas that are PAS+. (right, n=5). Data are representative of 2 independent experiments and are shown as mean ± SEM. **P* < 0.05, ***P* < 0.01, ****P* < 0.001, by 1-way ANOVA with Tukey's post-hoc test (A-E, G, H), 2-tailed unpaired t test (I-L, N, O) and 2-way repeated measures ANOVA with Bonferroni post-hoc test (F, M).

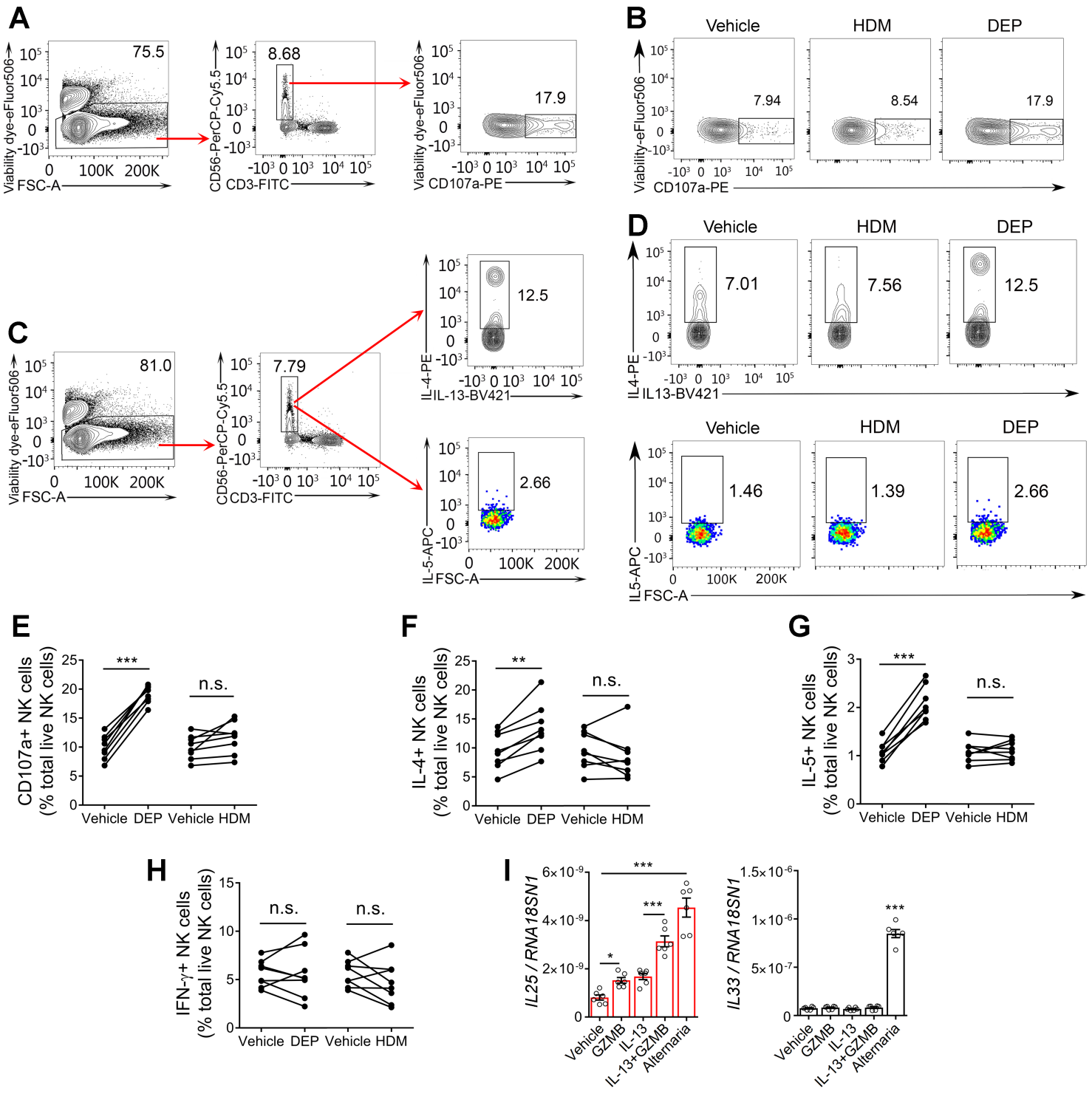

Figure 11. The NK cell pathway in human cell systems

(**A-H**) Human cord blood mononuclear cells (CBMCs) were incubated with DEP, HDM or vehicle (PBS) for 48 hours. To measure NK cell degranulation, PE-labeled anti-CD107a or isotype control IgG, monensin and brefeldin A were then added for additional 5 hours. To measure intracellular cytokines in NK cells, monensin

and brefeldin A were added for additional 4 hours. Cells were then stained with eFluor506 (viability) and antibodies for NK cell surface markers ± antibodies for cytokines. (**A, C**) Gating strategy to define degranulated (A) and cytokine-producing (C) NK cells. Lymphocytes (from the FSC-A vs. SSC-A plot) were gated on singlets and then on live cells (eFluor506$^-$). eFluor506$^-$ single lymphocytes were analyzed for CD56 and CD3. NK cells (CD56$^+$CD3$^-$) were analyzed for CD107a (marking degranulated cells; A) or intracellular cytokines (C). (**B, D**) Representative FC plots showing anti-CD107a labeling of NK cells (B) and anti-cytokine labeling of NK cells (D) under three stimulation conditions (DEP, HDM and vehicle). (**E-H**) Percentages of degranulated (CD107a$^+$) NK cells (E), IL-4$^+$ NK cells (F), IL-5$^+$ NK cells (G) and IFNγ$^+$ NK cells (H) in total live NK cells. n=8 subjects. (**I**) Levels of *IL25* and *IL33* mRNAs in human primary airway epithelial cells treated with vehicle (PBS), human granzyme B (GZMB) ± human IL-13, human IL-13 or an extract of Alternaria alternata; *RNA18SN1,* 18S ribosomal RNA. Data are pooled from eight independent experiments (E-H) or are representative of three independent experiments (I). Data are shown as mean ± SEM. **P* < 0.05, ***P* < 0.01, ****P* < 0.001 by 2-tailed paired t test (E-H) and 1-way ANOVA with Tukey's post-hoc test (I).